

Review Article

# A Critical Literature Review on Computer Vision Based Melanoma Detection and Identification

Soumya Gadag<sup>1</sup>, P. Pradeepa<sup>2</sup>

<sup>1</sup> Department of Electronics and Communication, S. G. Balekundri Institute of Technology, Jain Deemed to be University Karnataka, India

<sup>2</sup>Electrical and Electronics Engineering, Jain Deemed to be University, Kanakapura Campus Bangalore, Karnataka, India

<sup>1</sup>Corresponding Author : [soumya.gadag5@gmail.com](mailto:soumya.gadag5@gmail.com)

Received: 15 October 2022

Revised: 23 November 2022

Accepted: 08 December 2022

Published: 25 December 2022

**Abstract** - Melanoma is a skin tumor that initiates in the melanocyte cells that manage the pigmentation of the skin. Melanoma is still the most destructive form of skin cancer. In recent times, Convolutional neural network (CNN) centered classifiers have become quite popular for detecting melanoma. According to studies, CNN-based classifiers are equally accurate in classifying skin cancer scans as dermatologists. It has eased the process of Melanoma diagnoses. This work thoroughly assesses the most recent studies on the categorization of melanoma using deep learning and conventional machine learning procedures. The key purpose of this research is to compile cutting-edge research that identifies current research trends, problems, and prospects for melanoma diagnosis. It also looks into current approaches for applying deep learning to diagnose and identify melanoma. Finally, models, issues, and prospects have been provided to guide researchers working in the area of melanoma detection.

**Keywords** - Melanoma, Skin cancer.

## 1. Introduction

Conferring to a narrative from the World Health Organization, cancer is one of the primary reasons for mortality worldwide [1]. It suggests that there will be a substantial upsurge in the number of cancer patients in the upcoming time [2], [3]. If malignancy is identified and cured in its initial phases, the death rate of cancer patients can be decreased [4]. At present, the major concern of the researchers is to build a mechanism for the initial recognition of cancer. Melanoma is a very dangerous type of skin malignancy. It has been placed in 9th place among the most prevalent cancers. As shown in figure 1, Annually, more than 132,000 cases of cancer are detected worldwide [5]. As per the report of The American Cancer Organization in 2019, 192,310 melanoma cases were reported in the United States [5]. In the previous three decades, the highest incidence rate was 60 per 100,000 inhabitants in the USA and Australia. According to GLOBOCAN 2020 data, malignant melanoma is in the 32nd position in India in terms of annual incidence and is responsible for 3,916 patients (0.3% of all cases) [91], [92]. Contact with UV radiation from the sun is the main external source and the most significant external factor causing Melanoma [6][7][8].

However, if diagnosed promptly, melanoma can be treated with rapid excision [9, [10]]. Even with the help of skilled dermatologists, melanoma from skin lesions can be difficult and inaccurately identified utilizing techniques such as pictorial examination, medical testing, dermoscopic examination, surgery, and histological investigation of skin lesions [11] [12] [13]. This is because skin lesions have complicated visual features, including many sizes, multiple

forms, fuzzy borders, low contrast compared to surrounding skin, and noise, including skin hair, lubricants, bubbles, and air, as shown in figure 2

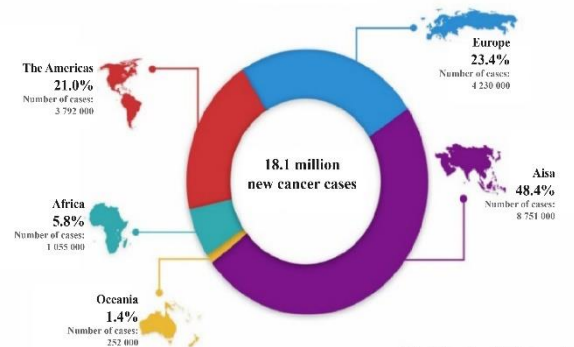


Fig. 1 Global cancer incidence

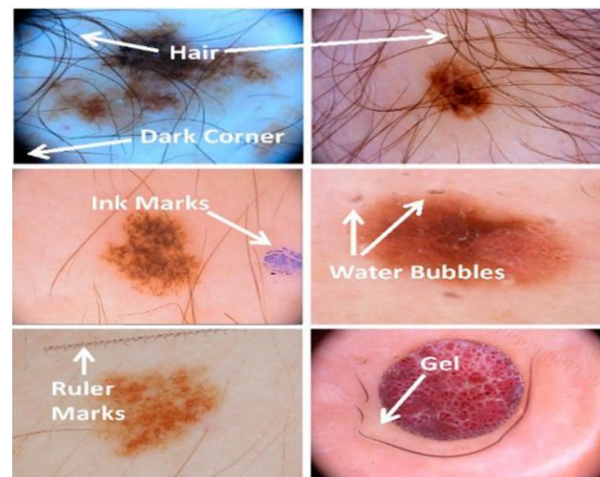


Fig. 2 Pictorial Representation of intricacy in skin lesion analysis



**1.1. Skin Cancer Classification**

Generally, cancer grows when DNA is broken, and our body cannot fix the mutilation. These damaged cells begin to multiply and divide abnormally. Such variations in the skin cause skin cancer [14]. Due to the rapid growth of these damaged cells, tumors are formed in the body. Skin cancer is easily identifiable as it develops in many layers of the skin, typically the epidermis. Distinctive skin types have different tendencies to grow skin malignancy. Its rate differs rendering on the type and color of skin, though it usually impacts the skin that is sensitive to sunlight. Also, genetic features have a significant function in the development of skin cancer. [93]. Skin cancers can be categorized as follows: (a) basal cell carcinoma, (b) squamous cell carcinoma, and (c) melanoma.

**1.1.1. Basal Cell Carcinoma**

This class of cancer starts in the basal cells — a specific kind of skin cell that substitutes dead skin cells with new ones. Though numerous forms of carcinoma exist, it frequently emerges as a tiny, marginally glowing lump on the skin [16]. Basal cell carcinoma commonly grows on skin that is open to sunlight, including the head and neckline. Long-term sun exposure is viewed as the main reason for the majority of basal cell carcinomas.

**1.1.2. Squamous Cell Carcinoma**

This skin malignancy commences in the squamous cells that make up the outer and middle layers of the skin [17]. Although it can be destructive, it often does not lead to life-threatening issues. If left untreated, squamous cell carcinoma of the skin can expand significantly or extend to other areas of your body, leading to life-threatening consequences.

**1.1.3. Melanoma**

The most perilous category of skin cancer, grows in the cells (melanocytes) that yield melanin.

The color of the skin depends on melanin. As well, melanoma can grow in the eyes and, infrequently, inside the body, such as in the nose or throat [18].

Still, with a significant cure rate, melanoma is the most treatable malignancy if identified in the primary phases [19]. Therefore, there should be a computerized diagnostic system to ease the timely detection of melanoma. The common steps of the many artificial vision system concepts include image procurement, pre-processing, segmentation, feature mining, selection, and classification [20]. Moreover, as shown in figure 3, the visual distinctions between benign skin lesions and melanoma can be quite minor, making it challenging for even skilled medical professionals to make the distinction between the two situations.

Therefore, evolving an effective Computer-Aided Diagnosis(CAD) system is necessary to identify and diagnose melanoma malignancy. It will increase the rate of melanoma discovery and timely identification, which can help with medication and lower the disease's fatality rate.

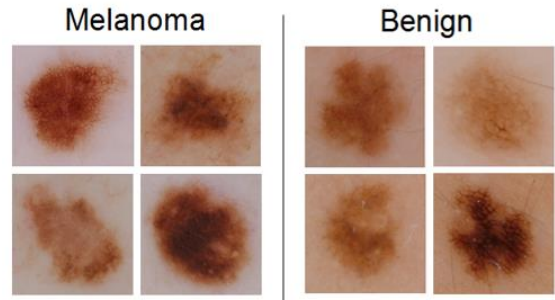


Fig. 3 visual equivalence between melanoma and benign lesions (ISIC Dataset)

**1.2. Dermoscopy and CAD for Melanoma Detection**

The healing rate of melanoma can be good, but it should be handled in its primary stages. Numerous non-invasive skin imaging methods [36] were introduced, like dermatoscopy, digital camera images [45], multispectral imagery [46], MRI [47], OCT [48], ultrasound [49], confocal laser scanning microscopy (CLSM) [50] etc. Table 1 represents a comparative analysis of these imaging methods. The dermatoscopy technique is more effective than other skin imaging techniques for detecting skin cancer since it produces a magnified (usually by a factor of 10) image of the skin that is ordinarily invisible to the human eye.

Dermoscopy and computer-aided diagnosis technologies are presently employed in these applications on a massive scale. A delayed diagnosis of melanoma can be fatal for the patient due to its quick growth and tendency to spread to other areas of the body. [21]. In its advanced stages, melanoma cannot be treated well. Figure. 4 illustrates the portions of healthy skin and a part of skin affected by melanoma. The skin has 3 main layers: the outmost layer, which comprises 1st level squamous cells. The 2<sup>nd</sup> layer is made up of basal cells, and the deepest layer is made up of melanocyte cells [22].

Dermoscopy is a non-invasive procedure that examines the skin's sub-surface structures using incident light beams and perhaps specific oil baths. Dermoscopy is a better method of melanoma detection than a non-assisted one, but a dermatologist's training still makes a difference in making a proper diagnosis [22].

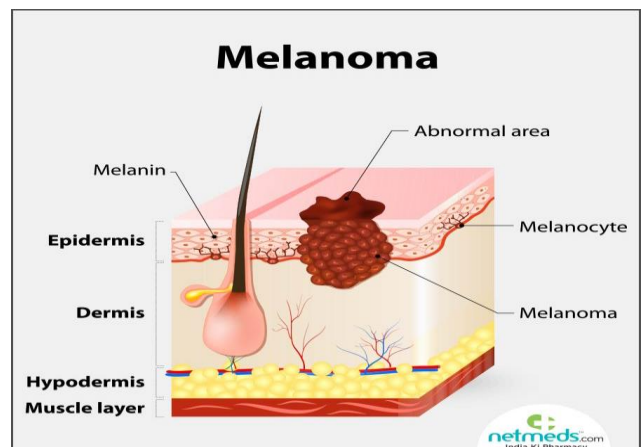


Fig. 4 Healthy and melanoma skin

Table 1. Information about several imaging methods for skin analysis

Imaging modalities	Advantages	Limitations	Penetration depth
<b>Dermatoscopy</b>	<ul style="list-style-type: none"> <li>High-quality</li> <li>Robust lighting system</li> <li>Deep Level of Visibility</li> <li>Eliminate reflection on the surface</li> </ul>	Skin superficial Layer	2mm
<b>Digital Camera</b>	<ul style="list-style-type: none"> <li>High-quality</li> <li>Resolution</li> </ul>	Limited morphologic information	0.1mm
<b>Multispectral imaging</b>	<ul style="list-style-type: none"> <li>Narrow frequency</li> <li>Consistency</li> </ul>	Absence of imaging in Z-coordinate and information about depth	0.1–1 mm
<b>Ultrasound</b>	<ul style="list-style-type: none"> <li>Ultrasound with High-frequency (100 MHz)</li> <li>Real-time examination</li> </ul>	Calculate penetration depth and skin thickness	1 mm
<b>MRI</b>	<ul style="list-style-type: none"> <li>Measure thickness or volume</li> <li>Tissue and Depth tissue information.</li> </ul>	MRIs cannot be performed on patients who have metal inside their bodies.	Total body infiltration
<b>OCT</b>	<ul style="list-style-type: none"> <li>High resolution</li> <li>Low coherence</li> <li>Tissue Design</li> <li>3D imaging</li> </ul>	Imperfect to tinny tumor cells (sturdily scattered epidermic tissue) Inadequate resolution	0.5–1.5 mm
<b>CLSM</b>	<ul style="list-style-type: none"> <li>High resolution Make 3-D design</li> </ul>	Tiny structures	0.3 mm

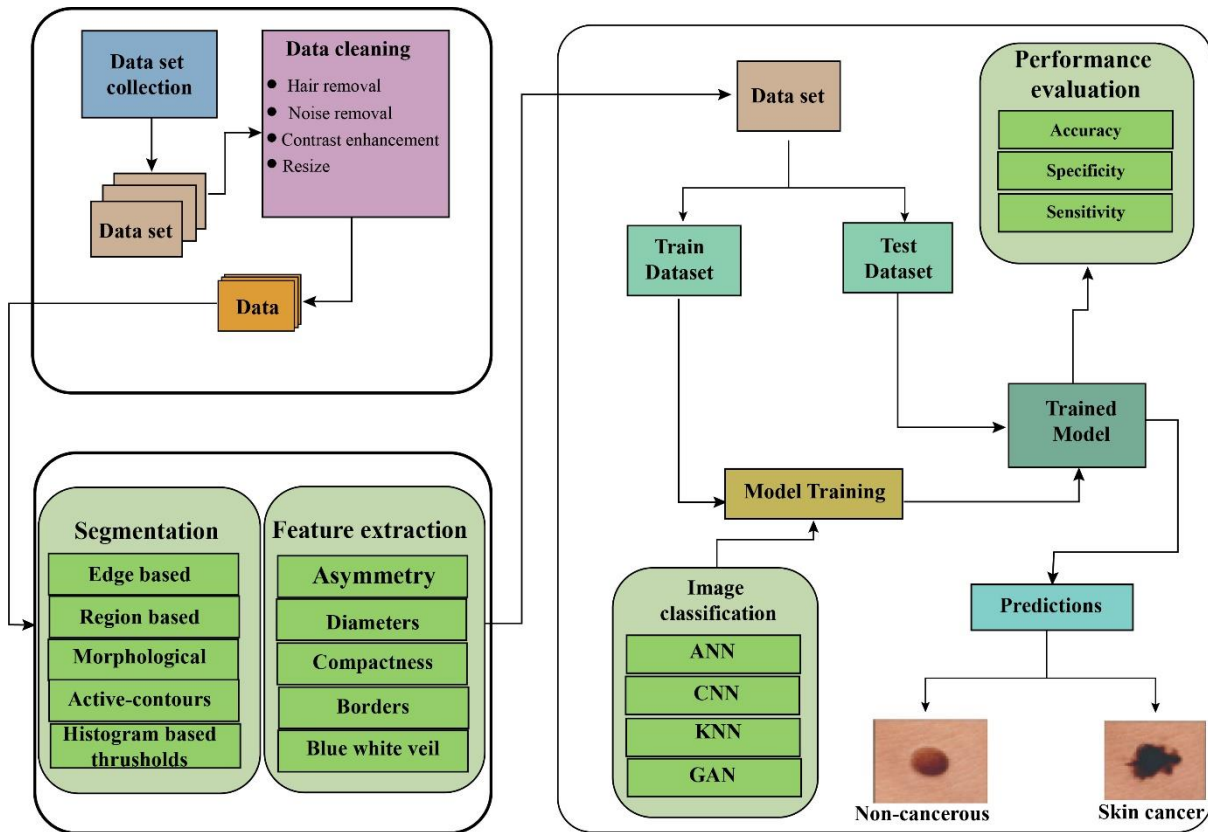


Fig. 5 Computer vision-based general procedure for skin cancer

Even when skilled dermatologists help with dermoscopy, differentiating melanoma from a normal lesion is difficult, particularly in the early stages. The accuracy of the melanoma diagnosis in these cases is considered to be between 75-84% [23]. Metrics like precision, sensibility, sensitivity, specificity, accuracy, etc., are typically used to assess the system's efficiency [94] [95]. Computer-aided diagnostics can help improve diagnosis precision and timeliness. In terms of color variation, asymmetry, and textural qualities, the computer can extract some information that may not be readily perceptible to the human eye. Numerous approaches based on computer vision have been published in this area of melanoma diagnosis.

Due to computer-based technology allows skin cancer symptoms to be diagnosed quickly, comfortably, and affordably. Numerous non-invasive approaches are suggested for examining skin cancer symptoms to determine if melanoma causes them or not. To identify skin cancer, a standard method is used: obtaining the image, pre-processing, segmenting the received pre-processed image, retrieving the required feature, and categorizing it, as illustrated in Figure 5

Most recent research is computer vision-based and based on deep learning. As a result, our primary focus is on deep learning-based melanoma detection methods. Deep learning has recently transformed the scene of machine learning (ML) approaches. It is regarded as a state of art ML area focusing on ANN techniques [27]. Deep learning (DL) methods are used in a range of contexts, including speech recognition [28], pattern recognition [29,32], cloud computing [33] and bioinformatics [30]. Deep learning systems have delivered promising outcomes in these areas compared to other conventional machine learning (ML) techniques. Recently, a variety of DL techniques have been applied in automatic skin tumor screening. In this article, we thoroughly examine DL-based methods for detecting skin cancer.

**1.3. Research Methodology**

This review aims to recognize the best existing classifiers, approaches, and datasets that depend on the DL technique for melanoma recognition. The systematic procedure of conducting a literature review aids in finding and evaluating the available research in the area of interest. The outcomes of the previous studies give logical evidence to create a the base for the categorization of appropriate research.

**1.4. Review Procedure**

In order to perform a systematic review, initially, we have started a review process. The Systematic Literature Review (SLR) process aids in defining the study topic, aims, and the most pertinent techniques for retrieving appropriate literature.

**1.5. Research Objectives**

The main aim of this article is as follows

- Emphasis on advanced research on conventional skin cancer detection techniques
- Emphasis on cutting-edge research on DL methods employed for melanoma diagnosis
- To highlight current trends, obstacles, and possibilities in the area of melanoma identification
- Examine the current methods for diagnosis of melanoma and give a comprehensive evaluation of these methods based on their affinities and variances.

**1.6. Research Question**

A systematic review still needs to analyze the main research topics. After formulating the research topics, the analytical technique includes extracting relevant studies. These questions are elaborated on in table 2.

These questions can be answered by reading published work. The key goal of this study is to review the advanced approaches for melanoma diagnosis from the perspective of CNN-based frameworks.

**Table 2. This research review considers several research questions**

Q1.	What kind of DL-centered classifiers are employed for melanoma diagnosis?	This research question aims to categorize the most recent work on melanoma detection.
Q2	What are the potential problems faced by DL procedures for the finding of melanoma?	This question seeks to determine the benefits and drawbacks of current DL techniques.
Q3	What are performance indicators employed by classification techniques for melanoma diagnosis?	The evaluation measures such as True Positive (TP), also called Recall or Sensitivity, Error Rate, FP, TN, and Specificity. False Negative (FN), Precision, and ROC are used to determine the correctness of various research.
Q4	What kinds of datasets are accessible for melanoma diagnosis?	This research aims at the accessibility of standard datasets. The amount of images accessible for training and testing in all datasets are also examined.

## 2. Literature Survey

Every CADx for skin cancer recognition includes similar stages: pre-processing and segmentation of the image, attribute selection, mining, and categorization (Abbas et al., 2018). Melanoma cancer has uneven boundaries, color disparity, irregular, crossed diameter, and coarse boundaries. The accurate identification of melanoma can be made with the help of feature selection and extraction. Using computer vision-based schemes of feature patterns, we can classify skin cancer identification techniques as (a) conventional ML algorithms of feature mining and categorization and (b) DL-centred approaches with diverse architectures.

### 2.1. Conventional Machine Learning Methods

The common machine learning techniques are discussed in this section, where we investigate several handcrafted characteristics like color characteristics and texture characteristics and how they are used to identify melanoma. Over the past ten years, handcrafted features like SIFT(scale-invariant feature transform) [31] and LBP(local binary patterns) [34] have been employed extensively in computer-vision applications. As time goes on, researchers add more characteristics to their systems to do tasks more effectively.

#### 2.1.1. Color and Texture Features

Bestowing to Oliveira et al. [35], the most prominent elements of dermoscopic images are color and texture. Since the color of healthy skin can be distinguished from the color of malignant skin, color characteristics, also referred to as chromatic attributes, are generally applied in the healthcare profession for image examination [96]. Likewise, skin texture is a natural characteristic that contains information about the skin's design or pattern arrangement. Table 3 represents a comparative analysis of various methods based on color and texture. The texture characteristic illustrates the connection between the grey values of the image space and the spatial neighborhood pixels. Conferring to the survey, any texture has both statistical and regular disparity. Therefore, all attributes cannot be accurately analyzed by a single method. This research describes four types of texture analysis approaches: statistical approaches, model-based approaches, structural technologies, and transform-based strategies.

Color analysis assists in estimating the most important characteristics to recognize skin diseases. As a result, in this methodology [35], researchers concentrated on finding the optimal combination of characteristics to be extracted by utilizing multiple feature mining methodologies based on shape qualities, color variation, and texture assessment. In essence, a change in skin color is the first clue to distinguishing benign from malignant melanoma on dermoscopic images. Afza et al. [36] employed this theory for segmentation and defined that a brighter channel enrichment procedure regulates local contrast. Next, segmentation was conducted via a statistically normal

distribution method. In the feature mining stage, best matrices features (like histogram, optimum color, and gray level incidences) are mined, and covariance-centered fusion is accomplished. Afterwards, optimum features are taken using a binary grasshopper optimization method. Nasir et al. [37] anticipated a procedure for the categorization of melanoma and benign skin tumors. This procedure incorporates pre-processing, tumor segmentation, feature mining, assortment, and categorization. DullRazor performs pre-processing in the situation of hair removal, while tumor surface and color info are used to improve tumor contrast. A mixed methodology for lesion segmentation has been applied, and the findings are combined, utilizing the additive law of probability. Then, a serial-based technique extricates and merges attributes like color, texture, and HOG(Histogram of Oriented gradients)shape.

A unique Boltzman Entropy approach is then employed to implement the selection of the fused characteristics. The SVM(Support vector Machine) categorizes the relevant features. Oukil et al. [39] presented novel methods based on the texture and color of skin cancer. The system creates a reasonably precise mask for each lesion by an automated segmentation based on k-means. Feature mining measures the variation of the current and novel color and texture attributes. In order to obtain the best results, the features are processed through the different color spaces and later fed to the KNN(K-Nearest Neighbor), SVM and ANN(Artificial neural network) classifiers. Abedini et al. [40] described a novel feature extraction method that obtains the low-level properties using a global grid, layout, and pyramid paradigm. Next, several classifiers, including RF, DT, SVM, and Neural Networks, are used to analyze these patterns.

Additionally, color asymmetry characteristics are analyzed to distinguish between benign and malignant tumors. Proper color recognition and distribution are crucial for an appropriate finding of pigmented skin cancer [35]. Accurate recognition of color, the pigmentation degree, and the dispersion of the color within the skin tumor are the main constituents of a dermoscopy review. In dermoscopy scans, normally epidermis becomes white.

Melanin color is essential since it assists in distinguishing between chromatic and structural patterns. Cudek et al. [41] presented a computerized color recognition method in digital images for melanocytic skin cancers. Initially, they transformed the image to CIE L\*a\*b color space, and k-means clustering was performed for color recognition. Their primary innovation was using city block distance to determine the variance between colors. The color data collected through clustering creates the ABCD formula's color parameter.



**Table 3. Comparative analysis of prevailing methods based on color and texture strategies**

Ref	Diagnosis	Classification algorithm	Dataset Used	Outcome
Oliveira et al. [35]	Lesion Classification	Optimum-path forest classifier	1104 dermoscopic images	Accuracy=92.3%, Sensitivity = 87.5% Specificity = 97.1%
Afza et al. [36]	skin laceration segmentation and classification	Support Vector Machine (SVM)	PH2 and ISBI 2016	ISBI 2016 =93.80% ISBI 2017 = 93.70%,
Nasir et al. [37]	categorization of melanoma and benign skin tumors	SVM	PH2	sensitivity 97.7%, specificity 96.7%, accuracy 97.5%, and F-score 97.5%,
Oukil et al. [39]	Melanoma classification	K nearest neighbors, SVM, and ANN	PH2	Sensitivity = 99.25%, Specificity = 99.58%, Accuracy = 99.51%
Chatterjee et al. [42]	Melanoma skin lesions	Support vector machine	Dermoscopic Culture, Dermoscopic Atlas, PH2 database and ISIC: database.	Sensitivity = 97.63% Specificity=100% Accuracy =98.28%
Tumpa et al. [43]	Melanoma skin lesions	Neural Network (NN)	ISIC archives the PH2	accuracy = 97.7%

**Table 4. Contribution, Limitations, and advantages of the existing schemes**

Ref	Contribution	Advantage	Limitation
Oliveira et al. [35]	Combination of color- and texture-related features	Better accuracy even with 50% of extracted features by using the correlation-based selection	Ensemble or deep learning schemes can help to reduce the time and accuracy-related issues
Afza et al. [36]	Optimal feature selection and segmentation by using the statistical normal distribution, histogram, color, and GLCM features	The feature extraction process is optimized, and binary grasshopper helps to improve the feature selection	Time complexity, accuracy, and false negative rate for cubic SVM remain challenging issues.
Nasir et al. [37]	It performs pre-processing, segmentation, feature mining, selection, and categorization tasks.	Hair removal is improved by DullRazor, texture and color attributes are mined from the skin, and fused attributes are selected by applying the novel Boltzman Entropy method	categorization accurateness degrades due to minimum resemblance difference amid lesions
Oukil et al. [39]	It uses a mixture of color and texture attributes	Combination of different feature extraction such as RGB, HSV, Lab, XYZ, and YCbCr	Differentiating between normal and pigmented lesions.
Chatterjee et al. [42]	A combination of texture and morphological features is presented. The 2D wavelet packet decomposition technique is also used. SVM with recursive feature elimination is used for feature selection	Border irregularities are addressed to improve the feature extraction	Accuracy and complexity tradeoff
Tumpa et al. [43]	The highest Gradient Intensity method is used for hair removal, Numerous characteristics like LBP, ABCD, and GLCM are determined	Combined feature extraction for two different types of combined datasets is useful for improving learning performance.	The segmentation precision of the Otsu segmentation method can be improved

Alternatively, these descriptors are used in statistical approaches such as the GLCM(Gray-level co-occurrence matrix), a traditional second-order statistics technique, and the grey level histogram. A statistical method is used when a texture is arbitrary in nature, and its primitives or other texture elements are challenging to identify. Paradigm-based approaches have fractal and stochastic paradigms like autoregressive and GMRF(Gaussian Markov Random Field). The image was transformed using spatial frequency attributes using techniques including the Fourier, Gabor, and wavelet transforms [42]. Tumpa et al. [43] used the maximum Gradient Intensity technique as a pre-processing phase for hair removal and image enhancement. Next, the Otsu Thresholding procedure detaches skin lesions from the images. Feature mining phase mines various attributes like LBP, GLCM, and ABCD is computed from the segmented pictures that will be applied to train a NN. Table 4 describes the contribution and limitations of existing schemes.

The ABCD rule (threshold) [13] emerged as a straightforward paradigm that dermatologists, beginner skin doctors, and non-physicians adopt to analyze the characteristics of melanoma in its initial treatable phase, boosting the initial identification of melanoma. The ABCD rule (threshold) attributes are Irregularity, Boundary anomaly, Color diversification, and big diameter. The ABCD features offer an easy method for evaluating pigmented lesions that may require further evaluation by a specialist, which could lead to additional work involving dermoscopy, surgery, or both. The rule is destined to be applied daily by laypeople and primary care doctors (non-dermatologists) as a straightforward way to warn of the clinical characteristics of melanoma. It is designed to distinguish between pigmented lesions and thin tumors. It is observed that the grouping of the ABCD characteristics decides the dubious lesions and has better precision when applied in combination, specifically when all melanomas are not required to obtain all four characteristics. Table 5 defines the ABCD rules with scoring and factor. Table 6 elucidates the classes and results after using ABCD rules.

**Table 5. ABCD rules with conditions**

Conditions	Narrative	Factor	Scoring
<b>Asymmetry</b>	Contour, colors, and structure	1.3	0-2
<b>Boundaries</b>	Eight Segments	0.1	0-8
<b>Colors</b>	dark-brown, white, black, red, blue-grey, light-brown/tan	0.5	1-6
<b>Diameter</b>	More than 6 mm	0.5	1-5

**Table 6. Outcomes of ABCD rules**

Classes	TDS
Suspicious	Between 4.76 and 5.45
Melanoma	More than 5
Benign	Less than 4.76

## 2.2. Deep Learning-Based Methods

Machine learning uses two different categories of algorithms: supervised and unsupervised. Supervised procedures cope with label data in classification techniques such as naive Bayes, SVM, ANNs, RF (Random Forest), DT(Decision Tree), and linear, logistic, and polynomial regression. Unlabeled data is used in unsupervised algorithms like clustering (k-means, PCA (Principal Component Analysis), and hidden Markov models). Conventional machine learning methods cannot effectively retrieve hierarchical or higher-level features. Hence, deep learning is utilized to calculate them [44]. Deep learning is a particular category of ML technique that creates numerous layers that can recognize specific properties of the dataset using ordered layers of artificial neural networks (ANNs). The researchers do not have to manually mine characteristics from the image. Deep neural networks (DNN) have a substantial role in skin cancer recognition as these contain a group of interrelated nodes. Their interconnected neural design is comparable to that of the human brain. Their nodes work together to find solutions to specific issues. The NN is trained for particular tasks; next, they work as specialists in the domains in which they were trained. Various present deep learning paradigms are Mobilenet, ResNet, GAN(Generative adversarial networks), GoogLeNet, VGG(Visual Geometry Group), DenseNet, UNet, Xception, and AlexNet. This part defines the prevailing procedures based on these DL paradigms for skin cancer investigation, as shown in Table 7.

### 2.1.1. Alex-Net

The Alex\_Net architecture is designed by the combination of five convolution layers and 3 fully connected layers. Generally, the training time remains a noteworthy issue in these networks; therefore, it replaces the tanh function with Rectified Linear Units (ReLU) to minimize the training time. Moreover, this architecture uses multiple GPU(Graphics Processing Unit) based training where neurons are distributed to different GPUs to increase the training process. These characteristics of AlexNet make it a strong method for pattern recognition. The basic design of AlexNet is shown in the below-provided figure 6.

The anticipated technique uses transfer learning with pre-trained AlexNet. This work used randomly initialized weights of the final three replacement layers based on the values of the initial model. Qiao et al. [52] assumed the pre-trained adapted AlexNet design where the Batch Normalization layer is applied to train the data. Subsequently, the Extreme Learning Machine replaces the final few layers (ELM). A recently modified metaheuristic known as the Fractional-order Red Fox Optimization (FORFO) Algorithm is employed to provide greater efficiency in the ELM network.

The transfer learning approach was merged with AlexNet as the pre-trained paradigm. The suggested model autonomously extracts useful attributes from the input raw image for categorization. Consequently, it does away with difficult lesion segmentation and feature extraction processes.

**Table 7. Deep learning family and conforming design applied in skin analysis**

NN or Deep Learning Family	Architectures	Recent works
ResNet	ResNet34, ResNet50, ResNet101, ResNet152	[55] [57], [58],[59],[60]
Inception /GoogLeNet	Inception v2, Inceptionv3, inception v4, InceptionResNet-v2	[63][64]
Unet	ResUnet,Deep ResUnet	[69] [70] [71]
DenseNet	DenseNet121, DenseNet161, DenseNet169, DenseNet201	[74] [79]
GAN	GAN, SPGGAN, DCGAN, DDGAN, LAPGAN,PGAN	[74] [75] [76][77]
AlexNet	AlexNet	[51] [52] [53] [54] [56]
Xception	Xception	[79]
EfficientNet	EfficientNet, EfficientNetB5, EfficientNetB6	[77][79]
VGG	VGG16, VGG19	[54] [62] [66] [67]

**Table 8. Comparative analysis of AlexNet and ResNet Based methods**

Ref	Work done	Novelty	Dataset	Performance
<b>Hosny et al. [51]</b>	Multiclass lesion classification using AlexNet	transfer learning with pre-trained AlexNet	ISIC 2018	Accuracy= 98.70%, sensitivity= 95.60%, specificity= 99.27% and precision= 95.06%
<b>Qiao et al. [52]</b>	Skin cancer classification by using deep learning architecture	AlexNet is modified by incorporating the BN layer, and FORFO is used to optimize the output of ELM	ISIC dataset	Accuracy = 97.14%
<b>Ameri et al. [53]</b>	classify skin lesions into benign and malignant categories with pre-trained AlexNet	Complexity reduction during feature extraction and pattern learning	HAM10000	ROC=0.91, Accuracy=84%, Sensitivity = 81%, and Specificity of 88%
<b>Dorj et al. [54]</b>	pre-trained AlexNet with ECOC SVM classifier	The final layer of ECOC SVM improves the accuracy	Manually collected 3753 images	Accuracy= 94.2%, Sensitivity=97.83% Specificity= 90.74%
<b>Mahbod et al. [55]</b>	Lesion classification by using pre-trained deep feature generators like ResNet-18, AlexNet, VGG16	Three different models extract the deep feature, and finally, SVM classifiers are used, and outputs are fused to generate the final classification	ISIC 2017	ROC= 83.83% Accuracy= 97.55%
<b>ResNet works</b>				
Ref	Work done	Novelty	Dataset	Performance
<b>Hagerty et al. [57]</b>	Melanoma classification	knowledge transfer via a ResNet-50	ISIC 2018 challenge	Accuracy =0.94 AUC = 0.90
<b>Boulahia et al. [58]</b>	Skin cancer classification			
<b>Guo et al. [59]</b>	Skin lesion classification	The output of different classification modules is ensemble utilizing logistic regression	ISIC 2017	Accuracy= 82.4% AUC = 0.917
<b>Khan et al. [60]</b>	skin lesion classification	pre-trained ResNet DNN like RESNET-50 and RESNET-101 are applied for features mining	HAM10000, ISBI 2017, and ISBI 2016	Accuracy 89.8%, 95.60%, and 90.20% for three datasets, respectively



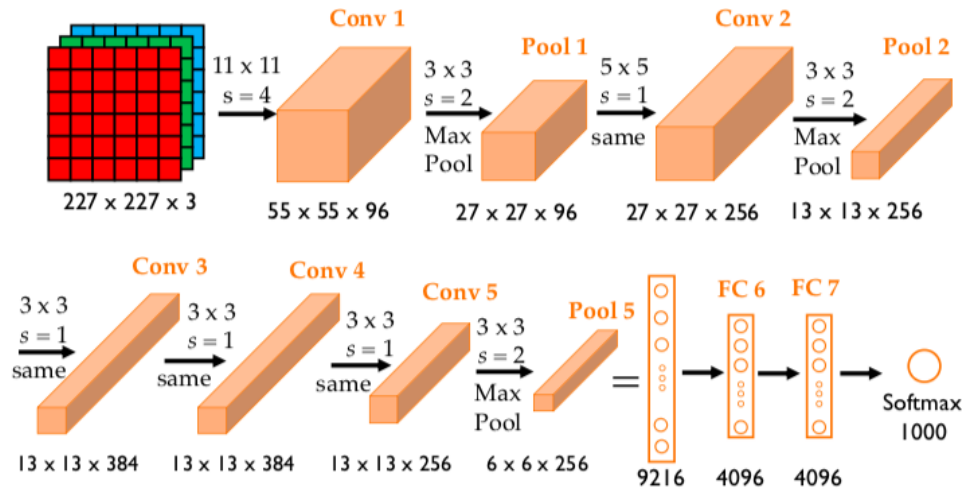


Fig. 6 AlexNet

Table 9. Explanation of prevailing methods for skin cancer study

Ref	Augmentation	Network	Advantage/Limitation
Hosny et al. [51]	Flipping and rotation	AlexNet uses 5 convolution layers and 2 FC layers, Dropout layers are constructed with the help of FC and softmax (same for transferred layers)	
Qiao et al. [52]		Pre-trained AlexNet is used for learning, and the last classification layer is substituted by ELM to obtain the classification	The BN helps to reduce the number of epochs for training
Ameri et al. [53]	NA	Resize image-> 227x227, SGDM algorithm for training, learning rate= 0.0001, and a mini-batch size = 30, 40 epochs.	Better ROC and compatibility for real-time analysis
Dorj et al. [54]	Cropping	5 convolution layers, 3 max pooling, and 7 strides are used. Finally, the ECOC SVM classifier is used	Future work suggested incorporating ABCD rules and developing of real-time system
Mahbod et al. [55]	0, 90, 180, and 270-degree augmentation and flipping augmentation	AlexNet, VGG16, and ResNet-18 for attributes and the outcome of the FC layer are given to SVM. The final output is fused	Fails to train the deeper features
<b>ResNet Works</b>			
Ref	Augmentation	Network	Advantage/Limitation
Hagerty et al. [57]	NA	A 2048 feature vector is produced as a result of a successive series of residual blocks with dimensionally increasing size after the input matrix. The final classification is done using a SoftMax operation after the feature vector is supplied to a fully connected network with 1000 nodes as its output.	Color features can be refined further, and augmentation can be included to generate the robust dataset
Boulahia et al. [58]	NA	An attention-based mechanism is combined with the ResNet	A better attention mechanism is discussed
Guo et al. [59]	Rotation, shift, flip	Two ResNet50 models process the pre-processed data and concatenate by using a fully connected layer	It uses local and global information of the image to incorporate the attention kind of scheme
Khan et al. [60]	NA	DCNN with kurtosis controlled principle component (KcPCA) to improve the feature extraction	Future work suggested incorporating a deep learning-based auto-encoder for feature extraction.

In some cases, the acquired images suffer from noise-related issues, degrading the diagnosis quality. Therefore, Dorj et al. [54] employed the pre-processing step to reduce the noise. Later, a pre-trained AlexNet CNN (Convolutional Neural Network) paradigm is employed for feature extraction. The categorization of skin cancer can be performed using an ECOC (error-correcting output coding) SVM classifier. Mahbod et al. [55] proposed a computerized method for skin tumor categorization, which applies optimized in-depth features from several standard CNNs and distinctive abstraction levels. The authors used three pre-trained deep prototypes, ResNet-18, VGG16, and AlexNet, as deep feature generators. The mined features are then employed to train SVM classifiers. The classifier outputs are merged in the final stage to obtain a classification. Table 8 describes the comparative analysis of AlexNet and ResNet. Hosny et al. [56] emphasized enhancing the efficiency of AlexNet by presenting a hybrid model that uses a pre-trained deep neural network (DNN) and transfers learning method, increasing the learning capacity. Transfer learning helps improve the performance of AlexNet by adjusting the weights, using SoftMax as a classification layer and enhancing the dataset with fixed and random rotation angles. Finally, the SoftMax layer is used to classify the lesions as melanoma and seborrheic keratosis.

### 2.2.2. ResNet (Residual Networks)

It is a conventional NN that works as the basis for numerous computer vision tasks. The well-known vanishing gradient issue occurs when gradients are repeatedly multiplied as they are back-propagated to earlier layers, so classic DNNs are challenging to train. Consequently, as the network becomes more complex, its performance becomes saturable or even declines quickly. ResNet employs skip connections to transfer output from one layer to another. This aids in reducing the issue of vanishing gradients. The ResNet50's basic framework is shown in the image below in figure 7.

According to Hagerty et al. [57], the image-processing components find aberrant pigment networks, color distributions, and blood vessels, which are lesion attributes similar to clinical dermoscopy information. Information provided to the pathologist in the clinical module comprises the patient's age, gender, tumor location, size, and background. The proposed approach's deep learning component adopts knowledge transfer with the help of the ResNet-50 network. Further, logistic regression is applied, which obtains the classification scores of every component from both processing modules to forecast an overall melanoma likelihood.

Boulaia et al. [58] concentrated on incorporating attention factors into deep learning systems for classifying melanoma. In fact, the idea of attention directs the learning process to concentrate on specific elements of the input image seen to be the most important. There are three primary phases to the suggested strategy. First, an advancement in the melanoma classification-specific transfer learning mechanism is described. Next, a basic

design variation is created that enables the integration of an additive attention method in a customized ResNet network. Lastly, this study examined the influence of the number of processes and where they are located in the melanoma classification design.

Guo et al. [59] suggest a feasible framework for skin cancer study: Multi-Channel-ResNet. The fundamental concept combines numerous ResNets, where the training data has been prepared using various techniques. They provide two training strategies for various scenarios with real-world applications. This approach outperforms a single ResNet or a straightforward assembly of ResNets.

Khan et al. [60] anticipated a computerized design for skin cancer categorization using transfer learning-based DNN attributes mining and KcPCA-based optimum attribute selection. The pre-trained ResNet DNNs like RESNET-50 and RESNET-101 are implemented for feature mining. After combining their information, they chose the best features to utilize as input for supervised learning techniques, including SVM and radial basis function (RBF) categorization. Table 9 briefly about the principal methods of skin cancer study.

### 2.2.3. GoogLeNet

GoogLeNet is a CNN system that is based on the Inception design. The network may select from a variation of convolutional filter sizes in all blocks owing to the use of Inception modules. These blocks are stacked on top of one another through an Inception network, with infrequent max-pooling layers with stride 2 that decrease the grid resolution in half, as shown in figure 8.

Yilmaz et al. [61] projected a CNN framework by adapting the GoogLeNet method. This paradigm augments a transposed convolutional layer along with a convolution layer in GoogLeNet. They intend to perform an up-sampling procedure using this deconvolution to keep some high-level information. According to Jayapriya et al. [62], the early detection of the disease with automatic melanoma diagnosis will significantly lower the fatality rate. Melanoma detection, skin lesion segmentation, and melanoma lesion identification are all carried out using a two-stage framework. Two FCNs (Fully Convolutional Networks) built on VGG-16 and GoogleNet are added to improve the segmentation performance. A mixed model is employed for integrating these two FCNs. A deep residual network (DRN) and manually created features were used to mine the feature from segmented lesions in the classification process. The SVM was used for categorization. Pham et al. [63] applied DCNN and data augmentation to enhance the classification efficiency of melanoma. They employed the Inception V4 design based on GoogleNet and attained an 89% classification rate. Esteva et al. [64] applied a single-trained full CNN to categorize skin cancers. They divided them into benign nevi, seborrheic keratoses, and melanomas. They employed Google's Inception v3 pertained design and managed a mediocre 72.1% classification performance. Using deep residual networks,

Yu et al. [65] demonstrated an automatic technique for melanoma identification in dermoscopy images. They solved the overfitting and degradation issues by using residual learning. A Fully (FCRN) was developed for

categorization. The outcomes of the studies reveal an accuracy of classification of 85.5%. A comparative analysis of the scheme based on VGG and GoogleNet is shown in Table 10.

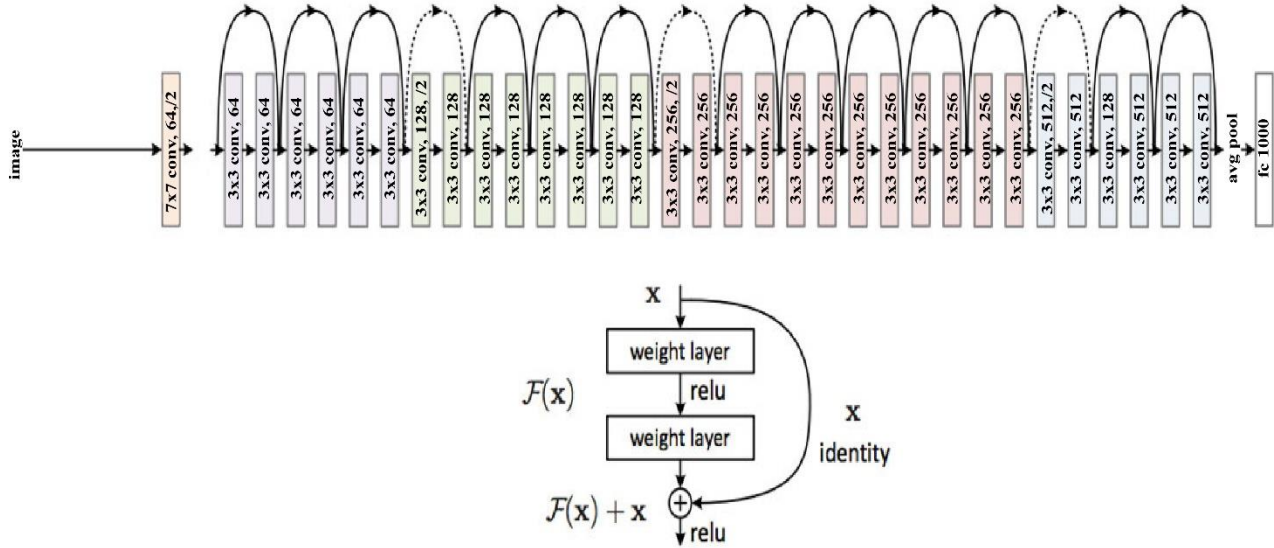


Fig. 7 ResNet50 Architecture

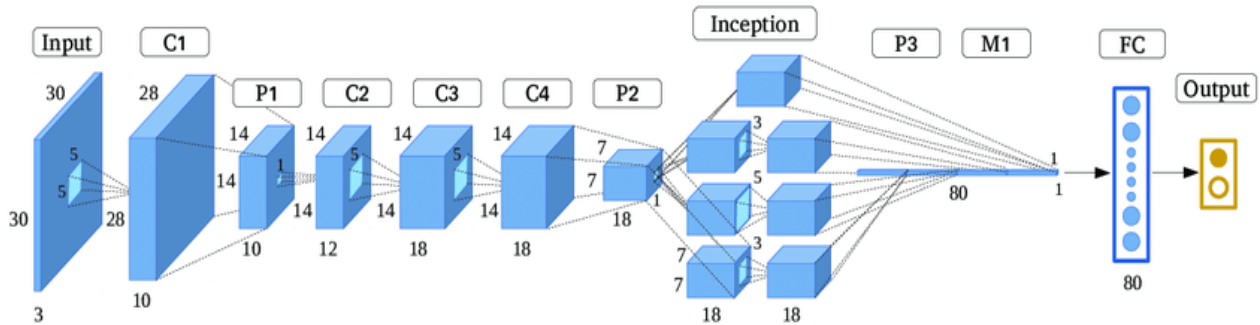


Fig. 8 GoogleNet Architecture

Table 10. Comparative analysis of existing schemes based on VGG and GoogleNet architectures

Ref	Work done	Novelty	Dataset	Performance
Yilmaz et al. [61]	skin cancer detection	Modified GoogLeNet	ISIC dataset	accuracy = 0.9309, sensitivity = 0.9739, kappa = 0.9620, F metric = 0.9620
Jayapriya et al. [62]	melanoma detection and skin lesion segmentation	Segmentation is improved by incorporating VGG-16 and GoogLeNet, and final classification is done by SVM	ISIC 2016 ISIC 2017 dataset	Accuracy = 0.8892 and 0.853 for both datasets, respectively.
Pham et al. [63]	skin lesion classification	Deep CNN	PH2 Dataset	AUC= 89.2%, AP=73.9% , ACC=89.0%
Esteva et al. [64]	skin lesion categorization	Pre-trained Inception v3		Accuracy =72.1%.
Yu et al. [65]	Skin cancer by using deep residual networks	Addressed the issue of overfitting and degradation	ISIC dataset	Accuracy = 0.855, AUC=0.783 AP =0.624 SE= 0.547 SP=0.931

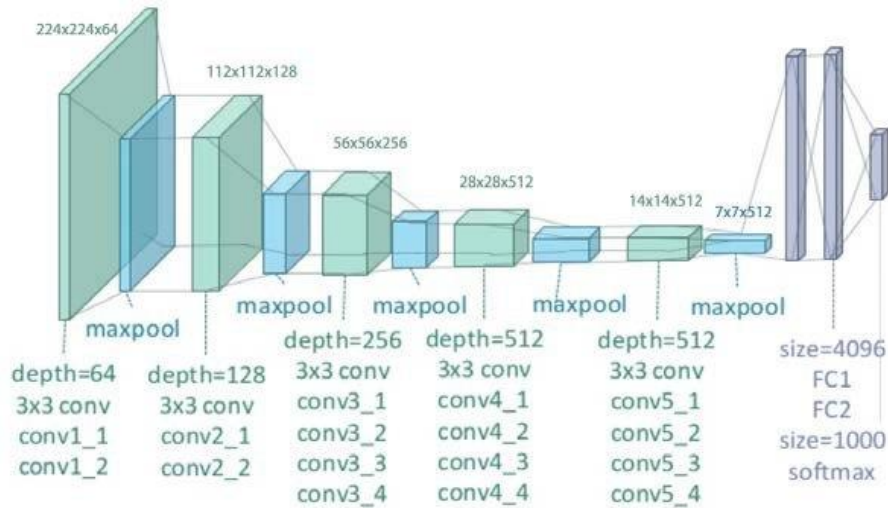


Fig. 9 VGG-19 model

### 2.2.4. VGG

Compared to earlier adaptations of AlexNet, which concentrated on reduced window widths and advancements in the first convolutional layer, VGG addresses depth, a crucial component of CNNs. A cutting-edge object-recognition model called VGG can acclimatize up to 19 layers. VGG, planned as a DCNN, performs better than baselines on several tasks and datasets beyond the ImageNet. VGG\_19 model is shown in figure 9.

According to [66], one of the most crucial factors in melanoma prognosis is thickness, which is also used to determine the surgical margin's size and to choose patients for sentinel lymph node surgery. Furthermore, there hasn't been much research done on measuring melanoma thickness from a clinical and computer-aided diagnostic standpoint. To solve this issue, we provide a useful ML tool to conduct the preoperative assessment of melanoma thickness. This method is unique in that it categorizes skin lesions into three classifications based on their thickness: less than 0.75 mm, 0.76-1.5 mm, and larger than 1.5 mm. In this research, they employ transfer learning of the VGG-19 (CNN) with an adjusted densely-connected classifier that has been pre-trained and tailored to the application. Due to the sparse data, they research the transfer learning method, which applies knowledge from a model trained on a distinctive task. Kaplan et al. [67] suggested a system based on pre-trained networks (i.e., VGG-16) and the DL algorithm categorize dermoscopic images. Yan et al. [68] suggested an attention-centered technique for melanoma identification. The attention components estimate attention maps highlighting visual regions of interest (ROI) important for lesion categorization. The attention components are trained along with other network parameters. Instead of only producing a class label. These attention maps offer a more understandable output. In addition, they suggest regularising attention maps with ROIs to make use of prior information (e.g., lesion segmentation or dermoscopic features). The categorization performance and the attention mappings can be improved when such prior knowledge is provided.

### 2.2.5. UNet

The semantic segmentation design is referred to as U-Net, as shown in figure 10. It has a long and contracting route. The contracting route is designed according to the basic CNN structure. A rectified linear unit (ReLU) and a 2x2 max pooling process with stride 2 for downsampling are applied after each application of two 3x3 convolutions (unpadded convolutions). They increase the number of feature channels by two after every cycle of downsampling. A 2x2 up convolution is applied here to upsample the features. This upconv reduces the feature channel by half. Further, a cropped feature map is connected to the contractual path and two 3x3 convolutions, each accompanied by a ReLU, at each stage of the expansive route. Owing to the loss of border pixels in each convolution, cropping is needed. Finally, a 1x1 convolution layer is used to map all feature vectors to the appropriate classes. Although deep learning models often produce outstanding segmentation performance for skin lesion segmentation, their application situations are limited by the high number of variables and FLOPs they require. Additionally, these systems do not effectively utilize low-level feature maps, which are crucial for anticipating specific information.

The Suggested EUnet-DGF retains a powerful encoding capability while using MBconv to construct its lightweight encoder.

Additionally, the depth-aware gated fusion block may combine feature maps of various depths and aid in predicting pixels on microscopic patterns [70]. Consequently, data imbalance continues to be a complex problem that affects the network's efficiency. Sella Veluswami et al. [71] implemented data augmentation to solve these challenges, followed by the CLAHE method for image enhancement. The lesions are segmented utilizing a neural network-based ensemble prototype that combines the segmentation algorithms of (FCN), SegNet, and U-Net to produce a binary image of the skin and the lesion, where the lesion is depicted with white and the skin is depicted with a black shade, allowing for the detection of only the damaged

lesion area. Various pre-trained networks, including Inception ResNet V2, Inception V3, Resnet 50, Densenet, and CNN, are used to classify these binary pictures further. The efficiency of the classification prototype is further

enhanced through a strategy that combines deep learning (DL) and machine learning (ML). In this hybrid model, the classification is carried out by DL models while the feature extraction is done by (SVM).

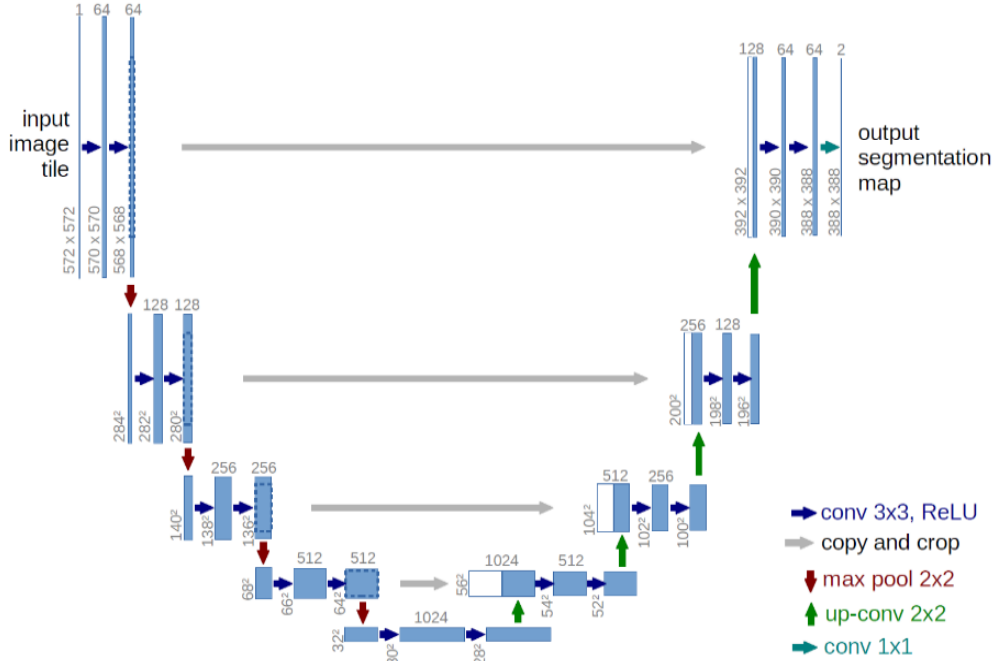


Fig. 10 U-Net

2.2.6. GAN (Generative Adversarial Neural Network) based Systems

It is a widely known classification method of DNN that is based on zero-sum game theory [72]. The GANs are based on the concept that two NNs compete to understand and capture variation in a database, like a discriminator and a generator. The generator unit is used to produce the sample data, as shown in figure 11. On the other hand, the discriminator module focus on discriminating between genuine and fraudulent data samples [73]. This process is repeated during the training process, and this competition leads to an increase in the performance of GAN. The main strength of a GAN network is its capacity to produce fake samples comparable to a real sample utilizing similar data distribution, like photorealistic photos.

Additionally, it can address the issue of inadequate training samples, a significant challenge for deep learning. Researchers have been employing numerous kinds of GANs, like Vanilla, condition GAN, DCNN-GAN, super-resolution GAN, and Laplacian Pyramid GAN. Currently, GANs are effectively being applied in skin malignancy diagnosis designs. Rashid et al. [74] recommended a skin cancer categorization method. The suggested technique added credible skin cancer images produced by GAN (Generative Adversarial Networks ) to a training batch of photographs. The discriminator unit utilized CNN as a separator, while the generator unit utilized a DCNN to classify various types of skin lesions. The results were compared with those of Residual network-50 and dense network. The Residual network-50, Dense Network and GAN model accuracy is 80%, 82% and 86 %, respectively,

for the classification of skin cancer. Deep learning procedures are accurate for massive, asymmetrical, and clean training datasets. For data purification, Bisla et al. [75] suggested a DL strategy and GAN for data augmentation. They employed dissociated DCNN-GANs to generate data. Dermoscopic images were classified into three subgroups, SK and nevus—via a pre-trained Residual network-50 prototype that was further enhanced with a filtered and extended dataset. The recommended system has 86 % accuracy, outpacing the reference point Residual network-50 method.

Based on PGAN(Prediction Generative Adversarial Network), an exclusive data expansion approach for skin cancer was also suggested [76]. Besides, the stabilizing strategy enhanced the generative system. In comparison to a non-augmented method's 67% accuracy, the suggested system's accuracy was 70.1%.

Efficient Attention Net, a CNN design proposed by Teodoro et al. [77], aims to detect melanoma and non-melanoma skin diseases in a timely manner. The approach shows the stages of the suggested categorization model's development and the benefits of each level. The hair surrounding the skin lesion is pre-processed out of the photos from the (ISDIS) collection in the first phase. The number of samples per class in the training set is then balanced using synthetic images created by a GAN prototype. A U-net model also generates masks for the images' interesting parts. Lastly, skin lesion classification using Efficient Attention Net training and the mask-based attention methodology.



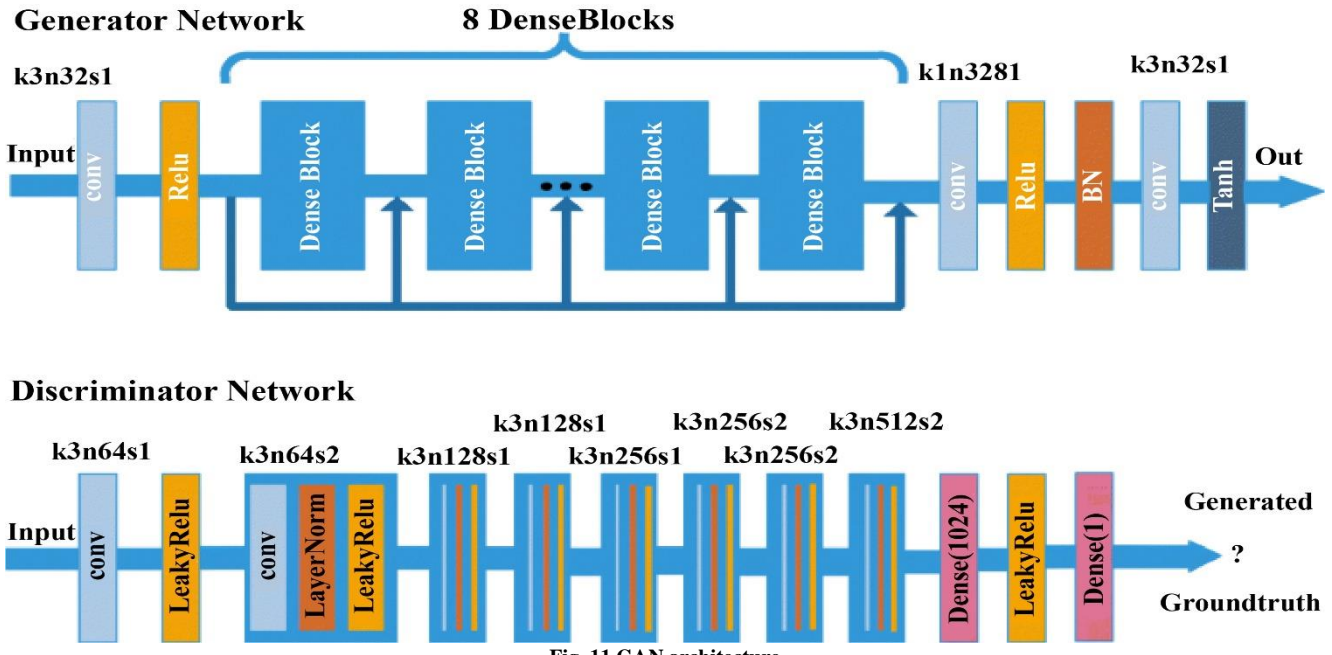


Fig. 11 GAN architecture

2.2.7. Other Deep Learning Techniques

Numerous computerized finding and recognition methods have been established so far. Their effectiveness has been constrained by the complicated visual properties of skin cancer images, which include irregular attributes and fuzzier borders. As previously mentioned, techniques based on DL and CNN have already been used to detect cancer. For automatic melanoma lesion recognition and segmentation.

Adegun et al. [78] offer a DL-based solution that gets over these restrictions. An upgraded encoder-decoder network with encoder and decoder sub-networks linked via a sequence of skip routes is suggested for efficient learning and feature retrieval. The semantic level of the encoder feature maps is increased by this network, approximating the decoder features map. This approach uses a multistage, multi-scale technology and a softmax classifier to categorize melanoma tumors pixel-by-pixel. As per the analysis of pixel-wise categorization, they developed a novel technique known as a "Lesion-classifier" that categorizes skin lesions into melanoma and non-melanoma. Deep CNN models are very accurate, but their "black-box" aspect stems from improper understandability, which limits their widespread application in clinical contexts.

Shorfuzzaman et al. [79] suggested an explicable CNN-based stacked collaborative paradigm to perceive melanoma skin lesions at former phases. The transfer learning theory has been applied in the collaborative stacking structure, where numerous CNN sub-models that accomplish the same classification job are commingled. The final predictions are produced by a new model known as a meta-learner using all the predictions from the sub-models. This model uses stacked ensemble classifiers (DenseNet121, Xception, and EfficientNetB0). A publicly available dataset with benign and malignant melanoma images is used to test the models.

Lafraxo et al. [80] emphasized automating the categorizing of dermoscopic images comprising skin cancers into malignant or benign. So, an enhanced DL-based system with a CNN was suggested. Further, this model uses dropout, regularisation, dropout, and data augmentation to minimize the impact of overfitting. Bhimavarapu et al. [81] incorporated DL procedures to automate melanoma identification from dermoscopic images.

A strategy for the prompt diagnosis of melanoma was presented by Xu et al. [82]. Image suppression, image segmentation, extraction of features, and categorization were all utilized sequentially. The segmentation approach used in the research was based on a (CNN) that has been tuned utilizing the satin bowerbird optimization (SBO). SBO was used to mine only crucial information from the segmented pictures. The images were finally categorized using (SVM) and the acquired features. The proposed strategy produced effective results when applied to the American Cancer Society database. Moreover, the suggested technique produced good results, and the combination of DL with the SBO algorithm resulted in a complicated system.

An automated melanoma classifier based on a DCN network is suggested by Kaur et al. [83] to differentiate between malignant and benign melanoma accurately. The DCNN's design was systematically created by arranging several layers in charge of retrieving low-level to high-level information from the skin images in a particular way. The assortment of various filters and their sizes, appropriate deep learning layers, selecting the depth of the network, and hyper-parameter optimization are other crucial factors in the design of DCNN. The main goal is to suggest a lightweight and less intricate Deep CNN than other cutting-edge approaches to classify melanoma skin malignancy effectively.



### 3. Dataset

There have been several suggested computerized approaches for the diagnosis of skin cancer. A strong and trustworthy dermoscopic image database is necessary to assess their diagnostic efficiency and anticipated confirmative outcomes. With the exception of pictures of nevi or melanoma lesions, different skin cancer databases have been small and lacking in variation. The tiny size of the datasets and the absence of different data make it challenging to train ANN for skin cancer classification. In spite of the fact that patients frequently have a range of non-lesions, preceding research for computerized diagnosis of skin tumors mostly concentrated on diagnosing melanocytic lesions, leading to an absence of diagnoses in the public datasets [84]. Thus, providing a uniform, trustworthy dataset of dermoscopic images is essential. Table 11 provides details about various datasets used for the study.

Table 11. dataset details used for the study

Sr.No.	Dataset Name	Year of issue	Total images
1	HAM10000	2018	10,015
2	PH2	2013	200
3	ISIC Collection	2016	25,331
4	DermQuest	1999	22,082
5	DermIS		6588
6	AtlasDerm	2000	1024
7	Dermnet	1998	23,000
8	ISBI Challenge 2016 Dataset	2016	1279
9	ISBI 2017 Dataset Challenge	2017	2000
10	2019 ISIC challenge	2019	25333
11	Dermofit Image Library		1300
12	MED-NODE dataset	2015	100

These datasets are briefly defined in the below-given sections:

#### 3.1. HAM10000 Dataset

It is a human-versus-machine dataset with 10,000 training images [84]. It solves the lack of diversity issue and is an open-access dataset on skin cancer images. The Dermatology Department of the Medical University of Vienna in Austria and Cliff Rosendahl's skin cancer center in Queensland, Australia, provided the 10,015 dermoscopic pictures that make up the final dataset of HAM10000. It took twenty years to put together this collection. Before digital cameras became widely used, photographic copies of lesions were submitted and kept at the Dermatology Department. These photographic prints were transformed into 8-bit color JPEG images with 300 DPI(Dots per inch) properties using a Nikon-Coolscan-5000-ED scanner. After the manual cropping, the resolution of the images was 800 X 600 pixels at a DPI of 72. The images were subjected to a variety of acquisition techniques and cleaning procedures,

and a partially automated workflow was created using a NN to achieve heterogeneity, as shown in figure 12 below.

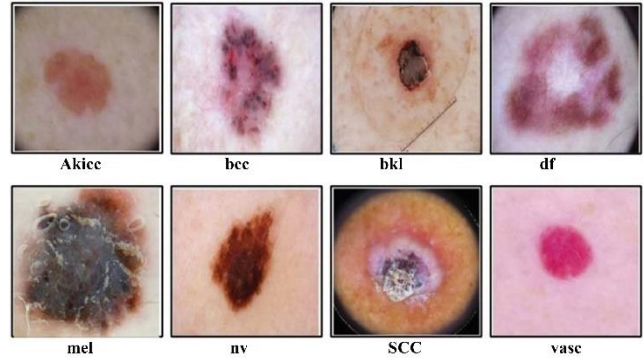


Fig. 12 Sample Images of the HAM10000 dataset

#### 3.2. PH2 Dataset

The Dermatology Center of Pedro Hispano Hospital in Portugal has the dermoscopic images for the PH2 dataset [85]. These pictures were taken with Tuebinger Mole-Analyzer equipment under identical circumstances and at a 20x magnification rate. The PH2 dataset includes 8-bit RGB color images with a small resolution. There are more than 150 dermoscopic images in the collection, 80 of which are common nevi, 80 of which are unusual nevi, and 40 of which are skin melanoma. This dataset includes clinical annotation of the lesion images, including pathological and medical diagnosis, assessment of several dermoscopic criteria, and medical segmentation of pigmented skin lesions. Dermoscopic criteria were used to accomplish the evaluation, including streaks, hues, regression zones, pigmented net, and whitish-blue veil blobs, as shown in figure 13.

Training and testing are separated into separate sections of the ISIC2016 repository. ISIC has nearly 1000 photos in its training subset and 380 dermoscopic pictures in its testing subset. Images from the two types of benign nevi and malignant melanomas are included. The collection contains images of melanoma tumors in about 30.3% of the images, while the other images are classified as benign nevi.

With time, ISIC includes more images in its collection and has created a strategy contest to create a computerized system for diagnosing skin cancer. Melanomas, seborrheic keratoses (SK), and benign nevi were the three image types added to the ISIC2017 dataset, which includes two thousand training photos, 150 images for validation, and 600 pictures for testing. The training dataset consists of 1372 pictures of benign nevi, 254 pictures of SK, and 374 pictures of melanomas. The validation dataset includes 30 photos of melanoma, 42 pictures of SK, and 78 images of benign nevi. The test dataset consists of 393 benign nevus pictures, 90 SK images, and 117 melanoma images. 12,594 training pictures, 100 validation pictures, and 1000 test images are added to ISIC2018. The ISIC2019 collection has a total of 25,331 photos, including eight skin lesion types, including BCC, Melanoma, melanocytic nevus, benign keratosis, AK, dermatofibroma, vascular lesion, and SCC. The ISIC2019 dataset contains image metadata, including the patient's gender, age, and position, as shown in figure 14.

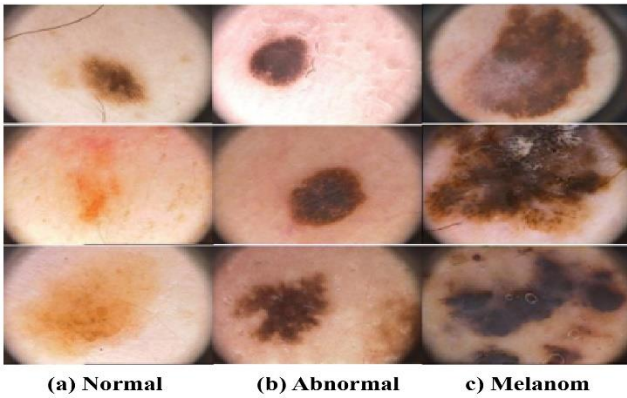


Fig. 13 Views of sample lesions in the PH<sup>2</sup> dataset

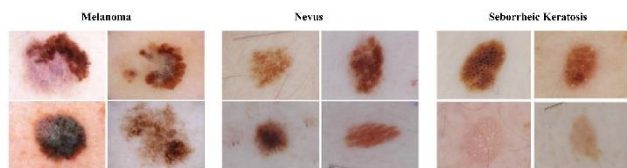


Fig. 14 Sample Images of the ISIC dataset

### 3.3. ISIC (International Skin Imaging Collaboration) Collection (ISIC2016, ISIC2017, ISIC2018, ISIC2019)

The ISIC collection [86] is a compilation of several databases on skin lesions. The ISIC made the first ISIC dataset in the 2016 (ISBI) challenge under the moniker ISIC2016.

### 3.4. DermQuest

22,082 dermoscopic images made up the DermQuest dataset, which was made available to the public [87]. Only the DermQuest dataset, out of all the dermoscopic datasets, has lesion tags for skin lesions. For every image in the collection, 134 lesion tags were present. In 2018, DermQuest's dataset was forwarded to Derm101. Unfortunately, now this dataset not is not available.

### 3.5. DermIS

The DermIS is the acronym for the dermatology information system [88]. It has approximately 6590 images. A pediatric dermatology online image atlas (PeDOIA) and a dermatology online image atlas (DOIA) have just been added to this dataset. Three thousand tumor photos representing about 600 dermatological diseases are included in the DOIA. It offers information on almost all sorts of skin illnesses, including dermoscopic pictures with multiple and preliminary diagnoses, case reports, and other details, as shown in Figure 15.

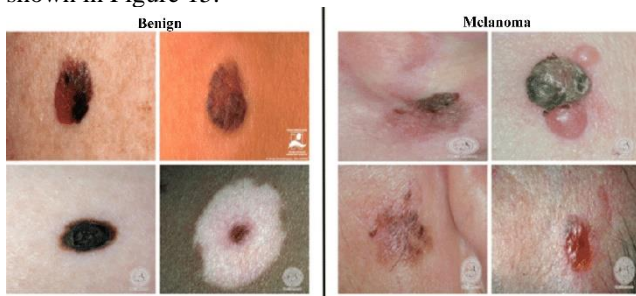


Fig. 15 View of DermIS image dataset

### 3.6. AtlasDerm

The dataset known as AtlasDerm represents the Atlas of Dermoscopy [89]. It is a special and well-structured mix of a book and graphics on a CD-ROM with training samples. It was initially created as a tool to aid medical professionals in identifying dermoscopic melanoma symptoms and diagnosing skin lesions. The AtlasDerm dataset considers numerous skin lesion cases, each with associated dermoscopic images. It has 30 photographs of arterial skin cancers, 275 images of melanocytic nevus, 582 images of melanoma, 70 images of benign keratoses, 70 images of benign cellular carcinoma, 5 images of dermatofibromas and 5 images of benign keratoses

### 3.7. Dermnet (Dermnet Skin Disease Atlas dataset)

Dr. Thomas Habif constructed the dermnet dataset in Portsmouth, New Hampshire, in 1998[90]. There are approximately 23,000 dermoscopic pictures available in this collection. Images of 643 skin conditions may be found in this database. The biological classification of these illnesses is divided into two levels. More than 600 skin conditions are in finer resolution on the bottom. Twenty-three different types of skin illnesses, including connective tissue illness, benign cancer, eczema, melanomas, moles, and nevi, are included in the top-level taxonomy.

## 4. Research Challenge

The categorization of melanoma is possible using a variety of datasets. While some datasets are accessible to the general public, others are not. Different datasets are found to have varying quantities of photos. Additionally, several authors formed their image dataset by using the internet.

### 4.1. Massive Training

The considerable training necessary for NN-based skin lexicon identification methods is one of the main hindrances. The system must undergo extensive training, a time-taking procedure that necessitates incredibly strong hardware to evaluate and comprehend the features from dermoscopic images correctly.

### 4.2. Dissimilarity in the Size of Tumors

The variability in lesion diameters is another problem. In the 1990s, a team of Italian and Austrian researchers gathered many pictures of malignant and benign melanoma lesions [73]. The lesions could be recognized with a diagnostic precision of up to 96% [75]. Yet, the diagnosis procedure was far more challenging and erroneous for small lesions at the early stages.

### 4.3. Images of Pale-Skinned Individuals in Common Datasets

Images of light-skinned people, especially from Europe, Australia, and the United States, can be found in common dermoscopic datasets. A neural network (NN) needs to learn to consider skin tone to accurately identify skin cancer in those with dark skin [76]. However, this is only feasible if the NN views enough pictures of persons with dark skin while being trained. Consequently, datasets with enough lesion images of persons with dark and

light skin are needed to improve the reliability of skin cancer detection systems.

#### 4.4. Trivial Interclass Disparity in Skin Malignance Images

A medical image shows extremely little interclass variability; the variance between skin cancer pictures with melanoma and those without it is ominously smaller, for example, the variation between images of cats and dogs. Additionally, it might be quite challenging to distinguish between a birthmark and a melanoma. Some diseases produce lesions that are incredibly difficult to differentiate from one another. The task of image assessment and categorization is extremely difficult as a result of this limited variability [32].

#### 4.5. Imbalanced Skin Malignancy Datasets

The real-world datasets that are utilized to identify skin tumor are quite imbalanced. Each type of skin cancer has a substantially inconsistent quantity of pictures in the imbalanced dataset. It is challenging to make simplifications from the pictorial characteristics of the dermoscopic images since, for instance, they include many pictures of generic skin lesion types but just a few pictures of the unusual ones [12].

#### 4.6. Lack of Access to Robust Hardware

For the NN software to retrieve the specific elements of a lesion's image, vital for improving skin tumour diagnosis, robust hardware resources with high graphical processing unit capability are needed. One of the biggest obstacles to DL-based skin lesion diagnosis training is the absence of high computing power.

#### 4.7. The absence of Age-Based Separation of Images

Standards Datasets Skin malignancies of various sorts, including Merkel cell carcinoma, BCC, and SCC, were developed after age 65 [77]. Currently, available standard dermoscopic databases include pictures of children. However, sufficient pictures of persons older than 50 must be seen by NN to diagnose skin cancer in senior patients accurately.

#### 4.8. Use of Different Optimization Systems

The automated detection of skin cancer involves several highly important phases, including pre-processing and lesion edge recognition. To enhance the efficiency of computerized skin cancer diagnostic systems, many optimization methods, including artificial bee colony algorithm [78], ACO [79], SSO [80], and PSO [81], can be investigated.

#### 4.9. Study of Genetic and Environmental Aspects

Researchers have detected several genetic risk factors for melanoma, including pale complexion, light-colored eyes, red hair, a profusion of moles on the body, and a family background of skin cancer. The likelihood of developing skin cancer increases significantly when these genetic risk features are coupled with ecological dangers like prolonged exposure to UV light [82]. These elements

can be coupled with current DL techniques for improved efficiency.

## 5. Answers to the Research Question

### 5.1. Evaluation of rq1: What kind of Classifiers Based on DL Algorithms are Utilized to Diagnose Melanoma Cancer?

One of the most prevalent cancer types is melanoma. Many recent, in-depth research, novel methodologies, and algorithms have used deep learning to diagnose melanoma. In this article, we evaluated the many image categorization algorithms that are currently in use, with a particular emphasis on methods based on DL and conventional ML techniques. Feature extraction techniques like color, texture, GLCM and many others are used in conventional ML algorithms. On the other hand, DL systems don't need a particular feature-extracting method.

### 5.2. Evaluation of rq2: What Potential and Problems exist in DL Algorithms for Melanoma Diagnosis?

The precision of various investigations was determined through evaluation criteria like sensitivity, specificity, accuracy, and area under the curve. Every classifier's accuracy is evaluated using these criteria. Skin cancer classification and segmentation have significantly improved thanks to DL systems. The lack of powerful hardware, the absence of age-wise division of pictures, the inclusion of light-skinned people in common datasets, small interclass dissimilarity in skin malignancy pictures, imbalanced skin malignancy datasets, and other issues are only a few of the difficulties this field faces.

### 5.3. Evaluation of rq3: What Performance Metrics are Used by Classification Approaches in Diagnosing Melanoma?

The accuracy (Acc) symbol stands for the rate of proper classification. It is determined by dividing the total number of predictions by the percentage of true predictions. It can be articulated as:

$$Acc = \frac{TP+TN}{TP+TN+FP+FN} \quad (1)$$

The model's sensitivity assessment is a different parameter. One can estimate the genuine positive rate measurements by identifying the proper classification. This can be articulated as

$$Sensitivity = \frac{TP}{TP+FN} \quad (2)$$

The subsequent parameter is the genuine negative rate, which is calculated and can be stated as follows:

$$Specificity = \frac{TN}{TN+FP} \quad (3)$$

Next, we have computed the precision of the suggested method. It is calculated by considering the ratio of True Positive and (True and False) positives.

$$P = \frac{TP}{TP+FP} \quad (4)$$

Conclusively, F-measure is estimated as the mean of precision and sensitivity performance. It is articulated as follows:

$$F = \frac{2 * P * \text{Sensitivity}}{P + \text{Sensitivity}} \quad (5)$$

#### 5.4. Evaluation of rq4: What Type of Datasets are Accessible for Detecting Melanoma?

There were numerous data sets accessible for the recognition of skin lesions, such as HAM10000, PH2, ISIC Archive, DermQuest, DermIS, AtlasDerm, Dermnet, etc. some of the datasets are having less number of images; therefore, data augmentation methods are applied. This also helps in improving the robustness of the deep learning system.

## 6. Conclusion

Modern melanoma detection research has been reviewed in this study. Furthermore, open problems and

difficulties have been noted. Also, this study examined in-depth a number of deep learning-based approaches to identify a melanoma, including fully CNN, pre-trained paradigm, ensemble, and handmade strategies. It has been noted that complicated and composite pre-processing methods like image resizing, cropping, and pixel value normalization is unnecessary when utilizing deep learning algorithms. Reviewing applicable articles has provided an anticipated taxonomy and an anticipated model.

Additionally, this analysis identifies the fundamental flaws in the current approaches and highlights the areas that still require development. The future study must make use of a larger dataset and fine-tune hyper-parameters to lower the likelihood of overfitting. In order to attain great accuracy, CNN must also learn how to collect data from persons with a dark complexion.

## References

- [1] Niccolò Nami et al., "Teledermatology: State-of-the-Art and Future Perspectives," *Expert Review of Dermatology*, vol. 7, no. 1, pp. 1-3, 2012. *Crossref*, <https://doi.org/10.1586/edm.11.79>
- [2] "Cancer in Australia 2017," Cancer Series no. 101. Cat. no. CAN 100, Australian Institute of Health and Welfare, 2017.
- [3] International Skin Imaging Collaboration, ISIC, 2019. [Online]. Available: <https://challenge2019.isic-archive.com>
- [4] American Skin Cancer Organization, Skin Cancer Information, 2019. [Online]. Available: <https://www.skincancer.org/skin-Cancer-Information/Skin-Cancer-Facts>.
- [5] FWHO, Ultraviolet Radiation, 2019. [Online]. Available: <http://www.who.int/uv/faq/skincancer/en/index1.html>
- [6] Ashley Sample, and Yu-Ying He, "Mechanisms and Prevention of UV-Induced Melanoma," *Photodermatology, Photoimmunology & Photomedicine*, vol. 34, no. 1, pp. 13-24, 2018. *Crossref*, <https://doi.org/10.1111/phpp.12329>
- [7] Jean Cadet, and Thierry Douki, "Formation of UV-Induced DNA Damage Contributing to Skin Cancer Development," *Photochemical & Photobiological Sciences*, vol. 17, no. 12, pp. 1816-1841, 2018. *Crossref*, <https://doi.org/10.1039/c7pp00395a>
- [8] Gerd P. Pfeifer et al., "Mechanisms of UV-Induced Mutations and Skin Cancer," *Genome Instability & Disease*, vol. 1, no. 3, pp. 99-113, 2020. *Crossref*, <https://doi.org/10.1007%2Fs42764-020-00009-8>
- [9] Lei Bi et al., "Automatic Skin Lesion Analysis Using Large-Scale Dermoscopy Images and Deep Residual Networks," *Computer Vision and Pattern Recognition*, vol. 2, 2017. *Crossref*, <https://doi.org/10.48550/arXiv.1703.04197>
- [10] Anthony F. Jerant et al., "Early Detection and Treatment of Skin Cancer," *American Family Physician*, vol. 62, no. 2, pp. 357-368, 2000.
- [11] Dr. M. Emre Celebi et al., "Automatic Detection of Blue-White Veil and Related Structures in Dermoscopy Images," *Computerized Medical Imaging and Graphics*, vol. 32, no. 8, pp. 670-677, 2008. *Crossref*, <https://doi.org/10.1016%2Fj.compmedimag.2008.08.003>
- [12] Qaisar Abbas et al., "Pattern Classification of Dermoscopy Images: A Perceptually Uniform Model," *Pattern Recognition*, vol. 46, no. 1, pp. 86-97, 2013. *Crossref*, <https://doi.org/10.1016/j.patcog.2012.07.027>
- [13] Adekanmi Adegun, and Serestina Viriri, "An Enhanced Deep Learning Framework for Skin Lesions Segmentation," *International Conference on Computational Collective Intelligence*, pp. 414-425, 2019. *Crossref*, [http://dx.doi.org/10.1007/978-3-030-28377-3\\_34](http://dx.doi.org/10.1007/978-3-030-28377-3_34)
- [14] Muhammad Imran Qadir, "Skin Cancer: Etiology and Management," *Pakistan Journal of Pharmaceutical Sciences*, vol. 29, no. 3, pp. 999-1003, 2016.
- [15] T. Tamilselvi et al., "Deep Derma Scan: A Proactive Diagnosis System for Predicting Malignant Skin Tumor with Deep Learning Mechanisms," *International Journal of Engineering Trends and Technology*, vol. 70, no. 8, pp. 310-317, 2022. *Crossref*, <https://doi.org/10.14445/22315381/IJETT-V70I8P232>
- [16] T. Chase, K. E. Cham and B. E. Cham, "Curaderm, The Long-Awaited Breakthrough for Basal Cell Carcinoma," *International Journal of Clinical Medicine*, vol. 11, no. 10, pp. 579-604, 2020. *Crossref*, <https://doi.org/10.4236/ijcm.2020.1110050>
- [17] Daniel E. Johnson et al., "Head and Neck Squamous Cell Carcinoma," *Nature Reviews Disease Primers*, vol. 6, pp. 1-22, 2020. *Crossref*, <https://doi.org/10.1038/s41572-020-00224-3>
- [18] M. Raza Zaidi, David E. Fisher, and Helen Rizos, "Biology of Melanocytes and Primary Melanoma," *Cutaneous Melanoma*, pp. 3-40, 2019. *Crossref*, [https://doi.org/10.1007/978-3-319-46029-1\\_42-1](https://doi.org/10.1007/978-3-319-46029-1_42-1)
- [19] Heinz Kutzner et al., "Overdiagnosis of Melanoma—Causes, Consequences and Solutions," *JDDG: Journal of the German Dermatological Society*, vol. 18, no. 11, pp. 1236-1243, 2020. *Crossref*, <https://doi.org/10.1111/ddg.14233>
- [20] Sharmin Majumder, and Muhammad Ahsan Ullah, "Feature Extraction from Dermoscopy Images for Melanoma Diagnosis," *SN Applied Sciences*, vol. 1, no. 7, pp. 1-11, 2019.

- [21] Andre G.C.Pacheco, and Renato A. Krohling, "The Impact of Patient Clinical Information on Automated Skin Cancer Detection," *Computers in Biology and Medicine*, vol. 116, p. 103545, 2020. *Crossref*, <https://doi.org/10.1016/j.combiomed.2019.103545>
- [22] Eugenio Vocaturo, Ester Zumpano, and Pierangelo Veltri, "Image Pre-Processing in Computer Vision Systems for Melanoma Detection," *In 2018 IEEE International Conference on Bioinformatics and Biomedicine (BIBM)*, pp. 2117-2124, 2018. *Crossref*, <https://doi.org/10.1109/BIBM.2018.8621507>
- [23] Siegel R. L et al., "Cancer Statistics," *CA: A Cancer Journal for Clinicians*, vol. 72, no. 1, pp. 7-33, 2022. *Crossref*, <https://doi.org/10.3322/caac.21708>
- [24] Akila Victor et al., "A Review on Skin Cancer Detection and Classification Using Infrared Images," *International Journal of Engineering Trends and Technology*, vol. 70, no. 4, pp. 403-417, 2022. *Crossref*, <https://doi.org/10.14445/22315381/IJETT-V70I4P235>
- [25] Nayana Banjan, Prajka Dalvi, and Neha Athavale, "Melanoma Skin Cancer Detection by Segmentation and Feature Extraction Using Combination of OTSU and STOLZ Algorithm Technique," *SSRG International Journal of Electronics and Communication Engineering*, vol. 4, no. 4, pp. 21-25, 2017. *Crossref*, <https://doi.org/10.14445/23488549/IJECE-V4I4P105>
- [26] Mehwish Dildar et al., "Skin Cancer Detection: A Review Using Deep Learning Techniques," *International Journal of Environmental Research and Public Health*, vol. 18, no. 10, p. 5479, 2021. *Crossref*, <https://doi.org/10.3390%2Fijerph18105479>
- [27] Nahata H, and Singh S. P., "Deep Learning Solutions for Skin Cancer Detection and Diagnosis," *Machine Learning with Health Care Perspective*, vol. 13, pp. 159-182, 2020. *Crossref*, [https://doi.org/10.1007/978-3-030-40850-3\\_8](https://doi.org/10.1007/978-3-030-40850-3_8)
- [28] Ali Bou Nassif et al., "Speech Recognition Using Deep Neural Networks: A Systematic Review," *IEEE Access*, vol. 7, pp. 19143-19165, 2019. *Crossref*, <https://doi.org/10.1109/ACCESS.2019.2896880>
- [29] Weibo Liu et al., "A Survey of Deep Neural Network Architectures and their Applications," *Neurocomputing*, vol. 234, pp. 11-26, 2017. *Crossref*, <https://doi.org/10.1016/j.neucom.2016.12.038>
- [30] Seonwoo Min, Byunghan Lee, and Sungroh Yoon, "Deep Learning in Bioinformatics," *Briefings in Bioinformatics*, vol. 18, no. 5, pp. 851-869, 2017. *Crossref*, <https://doi.org/10.1093/bib/bbw068>
- [31] Anusha Rao, and Kulkarni S. B., "A Hybrid Approach for Plant Leaf Disease Detection and Classification Using Digital Image Processing Methods," *The International Journal of Electrical Engineering & Education*, 2020. *Crossref*, <https://doi.org/10.1177/0020720920953126>
- [32] Vipul Sharma, and Roohie Naaz Mir, "Saliency Guided Faster-RCNN (SGFr-RCNN) Model for Object Detection and Recognition," *Journal of King Saud University-Computer and Information Science*, vol. 34, no. 5, pp. 1687-1699. *Crossref*, <https://doi.org/10.1016/j.jksuci.2019.09.012>
- [33] K. Siddesha, G. V. Jayaramaiah, and Chandrapal Singh, "A Novel Deep Reinforcement Learning Scheme for Task Scheduling in Cloud Computing," *Cluster Computing*, vol. 25, no. 6, pp. 1-18, 2022. *Crossref*, <http://dx.doi.org/10.1007/s10586-022-03630-2>
- [34] Kaplan Kaplan et al., "Brain Tumor Classification Using Modified Local Binary Patterns (LBP) Feature Extraction Methods," *Medical Hypotheses*, vol. 139, p. 109696, 2020. *Crossref*, <https://doi.org/10.1016/j.mehy.2020.109696>
- [35] Roberta B. Oliveira, Aledir S. Pereira, and João Manuel R. S. Tavares, "Computational Diagnosis of Skin Lesions from Dermoscopic Images Using Combined Features," *Neural Computing and Applications*, vol. 31, no. 10, pp. 6091-6111, 2019. *Crossref*, <https://doi.org/10.1007/s00521-018-3439-8>
- [36] Farhat Afza et al., "Microscopic Skin Laceration Segmentation and Classification: A Framework of Statistical Normal Distribution and Optimal Feature Selection," *Microscopy Research and Technique*, vol. 82, no. 9, pp. 1471-1488, 2019. *Crossref*, <http://dx.doi.org/10.1002/jemt.23301>
- [37] Muhammad Nasir et al., "An Improved Strategy for Skin Lesion Detection and Classification Using Uniform Segmentation and Feature Selection Based Approach," *Microscopy Research and Technique*, vol. 81, no. 6, pp. 528-543. *Crossref*, <https://doi.org/10.1002/jemt.23009>
- [38] Akhator Terence Azeke, and Dele Eradebamwen Imasogie, "The Tale of Malignant Melanoma, a Tertiary Hospital Experience in South-South, Nigeria," *SSRG International Journal of Medical Science*, vol. 5, no. 6, pp. 9-14, 2018. *Crossref*, <https://doi.org/10.14445/23939117/IJMS-V5I6P103>
- [39] Oukil S et al., "Automatic Segmentation and Melanoma Detection Based on Color and Texture Features in Dermoscopic Images," *Skin Research and Technology*, vol. 28, no. 2, pp. 203-2011, 2022. *Crossref*, <https://doi.org/10.1111/srt.13111>
- [40] Mani Abedini et al., "Accurate and Scalable System for Automatic Detection of Malignant Melanoma," *Dermoscopy Image Analysis*, 2015. *Crossref*, <http://dx.doi.org/10.1201/b19107-11>
- [41] Cudek P, and Hippe Z. S, "Melanocytic Skin Lesions: a New Approach to Color Assessment," *2015 8th International Conference on Human System Interaction (HSI)*, pp. 99-101, 2015. *Crossref*, <https://doi.org/10.1109/HSI.2015.7170650>
- [42] Saptarshi Chatterjee, Debangshu Dey, and Sugata Munshi, "Optimal Selection of Features Using Wavelet Fractal Descriptors and Automatic Correlation Bias Reduction for Classifying Skin Lesions," *Biomedical Signal Processing and Control*, vol. 40, pp. 252-262, 2018. *Crossref*, <https://doi.org/10.1016/j.bspc.2017.09.028>
- [43] Priyanti Paul Tumpa, and Md Ahasan Kabir, "An Artificial Neural Network Based Detection and Classification of Melanoma Skin Cancer Using Hybrid Texture Features," *Sensors International*, vol. 2, p. 100128, 2021. *Crossref*, <https://doi.org/10.1016/j.sintl.2021.100128>



- [44] Doaa A. Shoieb, Sherin M. Youssef, and Walid M. Aly, "Computer-Aided Model for Skin Diagnosis Using Deep Learning," *Journal of Image and Graphics*, vol. 4, no. 2, pp. 122-129, 2016. *Crossref*, <https://doi.org/10.18178/joig.4.2.122-129>
- [45] Luís Rosado et al., "From Dermoscopy to Mobile Tele dermatology," *Dermoscopy Image Analysis*, 2015. *Crossref*, <http://dx.doi.org/10.1201/B19107-13>
- [46] Ilona Kuzmina et al., "Towards Noncontact Skin Melanoma Selection by Multispectral Imaging Analysis," *Journal of Biomedical Optics*, vol. 16, no. 6, p. 060502, 2011. *Crossref*, <http://dx.doi.org/10.1117/1.3584846>
- [47] Bernard Querleux et al., "Quantitative Magnetic Resonance Imaging of the Skin: in Vitro and in Vivo Applications," *Imaging Technologies and Transdermal Delivery in Skin Disorders*, pp. 341-369. *Crossref*, <http://dx.doi.org/10.1002/9783527814633.Ch14>
- [48] Ali Rajabi-Estarabadi et al., "Optical Coherence Tomography Imaging of Melanoma Skin Cancer," *Lasers in Medical Science*, vol. 34, no. 2, pp. 411-420, 2019.
- [49] Orlando Catalano et al., "Skin Cancer: Findings and Role of High-Resolution Ultrasound," *Journal of Ultrasound*, vol. 22, no. 4, pp. 423-431, 2019. *Crossref*, <https://doi.org/10.1007/S40477-019-00379-0>
- [50] Mihaela Adriana Ilie et al., "Current and Future Applications of Confocal Laser Scanning Microscopy Imaging in Skin Oncology," *Oncology Letters*, vol. 17, no. 5, pp. 4102-4111, 2019. *Crossref*, <https://doi.org/10.3892%2Fol.2019.10066>
- [51] Khalid M. Hosny, Mohamed A. Kassem, and Mohamed M. Fouad, "Classification of Skin Lesions into Seven Classes Using Transfer Learning with AlexNet," *Journal of Digital Imaging*, vol. 33, no. 5, pp. 1325-1334, 2020. *Crossref*, <https://doi.org/10.1007/s10278-020-00371-9>
- [52] Li Qiao et al., "Skin Cancer Diagnosis Based on a Hybrid Alexnet/Extreme Learning Machine Optimized by Fractional-Order Red Fox Optimization Algorithm," *Proceedings of the Institution of Mechanical Engineers, Part H: Journal of Engineering in Medicine*, 2022. *Crossref*, <https://doi.org/10.1177/09544119221075941>
- [53] Ameri A, "A Deep Learning Approach to Skin Cancer Detection in Dermoscopy Images," *Journal of Biomedical Physics & Engineering*, vol. 10, no. 6, pp. 801-806, 2020. *Crossref*, <https://doi.org/10.31661/jbpe.v0i0.2004-1107>
- [54] Ulzii-Orshikh Dorj et al., "The Skin Cancer Classification Using Deep Convolutional Neural Network," *Multimedia Tools and Applications*, vol. 77, no. 8, pp. 9909-9924, 2018. *Crossref*, <https://doi.org/10.1007/s11042-018-5714-1>
- [55] Amirreza Mahbod et al., "Skin Lesion Classification Using Hybrid Deep Neural Networks," *In ICASSP 2019-2019 IEEE International Conference on Acoustics, Speech and Signal Processing (ICASSP), IEEE*, pp. 1229-1233, 2019. *Crossref*, <https://doi.org/10.1109/ICASSP.2019.8683352>
- [56] Khalid M. Hosny, Mohamed A. Kassem, and Mohamed M. Fouad, "Classification of Skin Lesions Using Transfer Learning and Augmentation with Alex-Net," *PloS One*, vol. 14, no. 5, p. e0217293, 2019. *Crossref*, <https://doi.org/10.1371/journal.pone.0217293>
- [57] Jason R Hagerty et al., "Deep Learning and Handcrafted Method Fusion: Higher Diagnostic Accuracy for Melanoma Dermoscopy Images," *IEEE Journal of Biomedical and Health Informatics*, vol. 23, no. 4, pp. 1385-1391, 2019. *Crossref*, <https://doi.org/10.1109/JBHI.2019.2891049>
- [58] Said Yacine Boulahia, Mohamed Akram Benatia, and Abderrahmane Bouzar, "Att2ResNet: A Deep Attention-Based Approach for Melanoma Skin Cancer Classification," *International Journal of Imaging Systems and Technology*, vol. 32, no. 2, pp. 476-489, 2022. *Crossref*, <https://doi.org/10.1002/ima.22687>
- [59] Songtao Guo, and Zhouwang Yang, "Multi-Channel-ResNet: An Integration Framework towards Skin Lesion Analysis," *Informatics in Medicine Unlocked*, vol. 12, pp. 67-74, 2018. *Crossref*, <https://doi.org/10.1016/j.imu.2018.06.006>
- [60] Muhammad Attique Khan et al., "Multi-Model Deep Neural Network Based Features Extraction and Optimal Selection Approach for Skin Lesion Classification," *In 2019 International Conference on Computer and Information Sciences (ICIS), IEEE*, pp. 1-7, 2019. *Crossref*, <https://doi.org/10.1109/ICISci.2019.8716400>
- [61] E Yilmaz, and M. Trocan, "A Modified Version of Googlenet for Melanoma Diagnosis," *Journal of Information and Telecommunication*, vol. 5, no. 3, pp. 395-405, 2021. *Crossref*, <https://doi.org/10.1080/24751839.2021.1893495>
- [62] Kalyanakumar Jayapriya, and Israel Jeena Jacob, "Hybrid Fully Convolutional Networks-Based Skin Lesion Segmentation and Melanoma Detection Using Deep Feature," *International Journal of Imaging Systems and Technology*, vol. 30, no. 2, pp. 348-357, 2020. *Crossref*, <https://doi.org/10.1002/ima.22377>
- [63] Tri-Cong Pham et al., "Deep CNN and Data Augmentation for Skin Lesion Classification," *In Asian Conference on Intelligent Information and Database Systems*, Springer, Cham, pp. 573-582, 2018. *Crossref*, [https://doi.org/10.1007/978-3-319-75420-8\\_54](https://doi.org/10.1007/978-3-319-75420-8_54)
- [64] Andre Esteva et al., "Dermatologist-Level Classification of Skin Cancer with Deep Neural Networks," *Nature*, vol. 542, no. 7639, pp. 115-118, 2017. *Crossref*, <https://doi.org/10.1038/nature21056>
- [65] Lequan Yu et al., "Automated Melanoma Recognition in Dermoscopy Images via Very Deep Residual Networks," *IEEE Transactions on Medical Imaging*, vol. 36, no. 4, pp. 994-1004, 2017. *Crossref*, <https://doi.org/10.1109/TMI.2016.2642839>
- [66] Joanna Jaworek-Korjakowska, Pawel Kleczek, and Marek Gorgon, "Melanoma Thickness Prediction Based on Convolutional Neural Network with VGG-19 Model Transfer Learning," *In Proceedings of the IEEE/CVF Conference on Computer Vision and Pattern Recognition Workshops*, pp. 2748-2756, 2019. *Crossref*, <https://doi.org/10.1109/CVPRW.2019.00333>
- [67] Ali Kaplan et al., "Prediction of Melanoma from Dermoscopic Images Using Deep Learning-Based Artificial Intelligence Techniques," *In 2019 International Artificial Intelligence and Data Processing Symposium (IDAP), IEEE*, pp. 1-5, 2019. *Crossref*, <https://doi.org/10.1109/IDAP.2019.8875970>



- [68] Yiqi Yan, Jeremy Kawahara, and Ghassan Hamarneh, "Melanoma Recognition via Visual Attention," *In International Conference on Information Processing in Medical Imaging*, Springer, Cham, pp. 793-804, 2019. *Crossref*, [https://doi.org/10.1007/978-3-030-20351-1\\_62](https://doi.org/10.1007/978-3-030-20351-1_62)
- [69] Tang Peng et al., "Efficient Skin Lesion Segmentation Using Separable-Unet with Stochastic Weight Averaging," *Computer Methods and Programs in Biomedicine*, vol. 178, pp. 289-301, 2019. *Crossref*, <https://doi.org/10.1016/j.cmpb.2019.07.005>
- [70] Xiangwen Ding, and Shengsheng Wang, "Efficient Unet with Depth-Aware Gated Fusion for Automatic Skin Lesion Segmentation," *Journal of Intelligent & Fuzzy Systems*, vol. 40, no. 5, pp. 9963-9975, 2021. *Crossref*, <https://doi.org/10.3233/JIFS-202566>
- [71] Sella Veluswami et al., "Melanoma Skin Cancer Recognition and Classification Using Deep Hybrid Learning," *Journal of Medical Imaging and Health Informatics*, vol. 11, no. 12, pp. 3110-3116, 2021. *Crossref*, <https://doi.org/10.1166/jmih.2021.3898>
- [72] Liang Gonog, and Yimin Zhou, "A Review: Generative Adversarial Networks," *In 2019 14th IEEE Conference on Industrial Electronics and Applications (ICIEA)*, IEEE, pp. 505-510, 2019. *Crossref*, <https://doi.org/10.1109/ICIEA.2019.8833686>
- [73] Ian Goodfellow, "NIPS 2016 Tutorial: Generative Adversarial Networks," *arXiv preprint arXiv:1701.00160*, 2016. *Crossref*, <https://doi.org/10.48550/arXiv.1701.00160>
- [74] Haroon Rashid, M. Asjid Tanveer, and Hassan Aqeel Khan, "Skin Lesion Classification Using GAN Based Data Augmentation," *In 2019 41st Annual International Conference of the IEEE Engineering in Medicine and Biology Society (EMBC)*, IEEE, pp. 916-919, 2019. *Crossref*, <https://doi.org/10.1109/EMBC.2019.8857905>
- [75] Devansh Bisla et al., "Towards Automated Melanoma Detection with Deep Learning: Data Purification and Augmentation," *In Proceedings of the IEEE/CVF Conference on Computer Vision and Pattern Recognition Workshops*, pp. 2720-2728, 2019. *Crossref*, <https://doi.org/10.1109/CVPRW.2019.00330>
- [76] Ibrahim Saad Ali, Mamdouh Farouk Mohamed, and Yousef Bassyouni Mahdy, "Data Augmentation for Skin Lesion using Self-Attention based Progressive Generative Adversarial Network," *arXiv e-prints*, arXiv-1910, 2019. *Crossref*, <https://doi.org/10.48550/arXiv.1910.11960>
- [77] Arthur A. M. Teodoro et al., "A Skin Cancer Classification Approach using GAN and RoI-Based Attention Mechanism," *Journal of Signal Processing Systems*, 2022. *Crossref*, <https://doi.org/10.1007/s11265-022-01757-4>
- [78] Adekanmi A. Adegun, and Serestina Viriri, "Deep Learning-Based System for Automatic Melanoma Detection," *IEEE Access*, vol. 8, pp. 7160-7172, 2019. *Crossref*, <https://doi.org/10.1109/ACCESS.2019.2962812>
- [79] Mohammad Shorfuzzaman, "An Explainable Stacked Ensemble of Deep Learning Models for Improved Melanoma Skin Cancer Detection," *Multimedia Systems*, vol. 28, no. 4, pp. 1309-1323, 2022. *Crossref*, <https://doi.org/10.1007/s00530-021-00787-5>
- [80] Samira Lafraxo, Mohamed El Ansari, and Said Charfi, "MelaNet: An Effective Deep Learning Framework for Melanoma Detection Using Dermoscopic Images," *Multimedia Tools and Applications*, vol. 81, no. 11, pp. 16021-16045, 2022. *Crossref*, <https://doi.org/10.1007/s11042-022-12521-y>
- [81] Usharani Bhimavarapu, and Gopi Battineni, "Skin Lesion Analysis for Melanoma Detection Using the Novel Deep Learning Model Fuzzy GC-SCNN," *In Healthcare*, vol. 10, no. 5, p. 962, 2022. *Crossref*, <https://doi.org/10.3390/healthcare10050962>
- [82] Zhiying Xu et al., "Computer-Aided Diagnosis of Skin Cancer Based on Soft Computing Techniques," *Open Medicine*, vol. 15, no. 1, pp. 860-871, 2020. *Crossref*, <https://doi.org/10.1515/med-2020-0131>
- [83] Ranpreet Kaur et al., "Melanoma Classification Using a Novel Deep Convolutional Neural Network with Dermoscopic Images," *Sensors*, vol. 22, no. 3, p. 1134, 2022. *Crossref*, <https://doi.org/10.3390/s22031134>
- [84] Philipp Tschandl, Cliff Rosendahl, and Harald Kittler, "The HAM10000 Dataset, a Large Collection of Multi-Source Dermoscopic Images of Common Pigmented Skin Lesions," *Scientific Data*, vol. 5, no. 1, pp. 1-9, 2018. *Crossref*, <https://doi.org/10.1038/sdata.2018.161>
- [85] Teresa Mendonça et al., "PH2 - A Dermoscopic Image Database for Research and Benchmarking," *In 2013 35th Annual International Conference of the IEEE Engineering in Medicine and Biology Society (EMBC)*, IEEE, pp. 5437-5440, 2013. *Crossref*, <https://doi.org/10.1109/EMBC.2013.6610779>
- [86] [Online]. Available: <https://www.isicarchive.com/#/topWithHeader/onlyHeaderTop/gallery?filter=%5B%5D>
- [87] Almut Boer, and KC Nischal, "A Growing Online Resource for Learning Dermatology and Dermatopathology," *Indian Journal of Dermatology Venereology and Leprology*, vol. 73, pp. 138-140, 2007. *Crossref*, <https://doi.org/10.4103/0378-6323.31909>
- [88] DermIS. [Online]. Available: <https://www.dermis.net/dermisroot/en/>
- [89] Giuseppe Argenziano et al., "Interactive atlas of Dermoscopy," EDRA Medical Publishing and New Media, Milan, Italy, 2000.
- [90] Dermnet. [Online]. Available: <http://www.dermnet.com/dermatology-pictures-skin-disease-pictures/>
- [91] Nour Kibbi, Harriet Kluger, and Jennifer Nam Choi, "Melanoma: Clinical Presentations," *Cancer Research and Treatment*, pp.107-129, 2016. *Crossref*, [https://doi.org/10.1007/978-3-319-22539-5\\_4](https://doi.org/10.1007/978-3-319-22539-5_4)
- [92] Bivas Biswas et al., "Not so 'rare'-An Example of Malignant Melanoma in India: Report from a Tertiary Cancer Centre," *Ecancermedicalscience*, vol. 15, p. 1335, 2021. *Crossref*, <https://doi.org/10.3332/ecancer.2021.1335>
- [93] Catarina Campos et al., "High-Throughput Sequencing Identifies 3 Novel Susceptibility Genes for Hereditary Melanoma," *Genes*, vol. 11, no. 4, p. 403, 2020. *Crossref*, <https://doi.org/10.3390/genes11040403>
- [94] Imran Razzak et al., "Skin Lesion Analysis Toward Accurate Detection of Melanoma Using Multistage Fully Connected Residual Network," *In 2020 International Joint Conference on Neural Networks (IJCNN)*, IEEE, pp. 1-8, 2020. *Crossref*, <https://doi.org/10.1109/IJCNN48605.2020.9206881>

- [95] Vatsala Anand et al., "An Automated Deep Learning Models for Classification of Skin Disease Using Dermoscopy Images: A Comprehensive Study," *Multimedia Tools and Applications*, vol. 81, pp. 37379–37401, 2022. *Crossref*, <https://doi.org/10.1007/s11042-021-11628-y>
- [96] Sameena Pathana K, Gopalakrishna Prabhu, and P.C.Siddalingaswamy, "Techniques and Algorithms for Computer Aided Diagnosis of Pigmented Skin Lesions—A Review," *Biomedical Signal Processing and Control*, vol. 39, pp. 237-262, 2018. *Crossref*, <https://doi.org/10.1016/j.bspc.2017.07.010>